Lawrence Berkeley National Laboratory

Title
LOCAL MODES OF BENZENE AND BENZENE DIMER STUDIED BY INFRARED-ULTRAVIOLET DOUBLE RESONANCE IN A SUPERSONIC BEAM

Permalink
https://escholarship.org/uc/item/7hd3x8z5

Authors
Page, R.H.
Shen, Y.R.
Lee, Y.T.

Publication Date
1987-09-01

Lawrence Berkeley Laboratory
UNIVERSITY OF CALIFORNIA

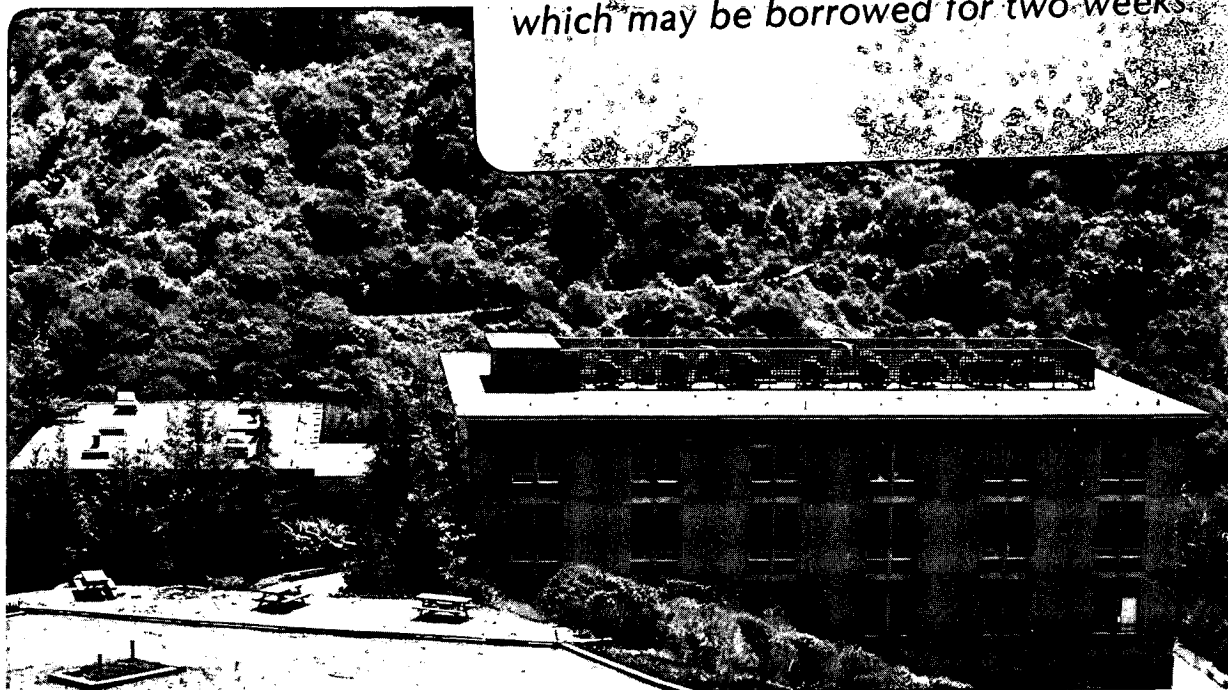## Materials & Chemical Sciences Division

Local Modes of Benzene and Benzene Dimer Studied by Infrared-Ultraviolet Double Resonance in a Supersonic Beam

R.H. Page, Y. R. Shen, and Y.T. Lee

September 1987

DISCLAIMER

LOCAL MODES OF BENZENE AND BENZENE DIMER STUDIED BY

INFRARED-ULTRAVIOLET DOUBLE RESONANCE IN A SUPERSONIC BEAM

Ralph H. Page,[*][(a)] Y. R. Shen,[*] and Y. T. Lee[†]

Materials and Chemical Sciences Division
Lawrence Berkeley Laboratory
Berkeley, California 94720

ABSTRACT

We used rotational cooling of molecules to ~ 5°K by supersonic

expansion and state-selective, multilevel saturation spectroscopy to

obtain high-resolution spectra of the fundamental and first and second

overtone transitions of C-H stretching modes in benzene and its dimer.

Greatly reduced linewidths (<3 cm^{-1} FWHM) in the rich spectra show that

previously reported spectra have suffered from inhomogeneous

congestion. Our observed spectral widths indicate that the vibrational

lifetimes of the C-H stretches are at least a few psec, even at the

energy of the second overtone (8800 cm^{-1}.) The "local mode" picture

appears to apply when at least 3 quanta of C-H stretching motion are

present. Spectra of the dimer are similar to those of the monomer but

show a red shift of a few cm^{-1}, the appearance of combination bands

involving van der Waals vibrational modes, some intensity changes, and

a broadening of spectral features that increases with the vibrational

energy. The dimer's predissociation lifetime at ~ 3000 cm^{-1}

vibrational energy exceeds ~ 3 psec.

I. INTRODUCTION

The familiar normal mode model has long been used to describe the vibrations of polyatomic molecules.[1,2] As a zeroth-order description, it works well as long as the anharmonic interactions between vibrational states are weak compared with the spacings between their energy levels. A general vibrational state can then be expressed as a superposition of normal-mode vibrations. But as the total vibrational energy is raised, the number of states, or ways it can be partitioned among the vibrational degrees of freedom, grows rapidly. The states may even become so closely spaced that they overlap and form a "quasicontinuum." Nearly-degenerate zeroth-order states become strongly mixed by the anharmonic interactions, so that the normal mode description is inappropriate. In general, each vibrational state is then a complex admixture of many zeroth-order states. The vibrational motion is quite complicated and energy is distributed throughout the molecule.

Local ("bond") modes provide a counterintuitive and fascinating contrast to this behavior. They are vibrational modes with long (hundreds of vibrational periods) lifetimes in which the motion (and energy) are more or less confined to a single bond. They can exist even when they are embedded in a dense manifold of other vibrational modes, sometimes referred to as a "bath."

By studying these "simple" local modes we hope to understand the vibrational behavior of molecules better. We want to know under what conditions local modes can exist, and what the details of their motions are. An important aspect of this problem is to understand the couplings between the local and other vibrational modes. These

2

couplings are responsible for the structured spectra, and decays of local mode vibrations. It is interesting to see how the effects of these perturbations change as the total energy and density of states vary.

The local mode description of vibrations was in use by 1936 [3] in order to explain the overtone absorption spectra of polyatomic molecules. Specifically, the study of local modes[4-7] has concentrated on overtones of stretching vibrations of O-H and C-H bonds. Their high fundamental stretching frequencies (above 3000 cm^{-1}) cause them to be far out of resonance with fundamentals involving more massive parts of a molecule, so that local behavior can stand out. In a molecule with several identical "oscillators" (O-H or C-H bonds), not all overtones of their stretches are purely local mode vibrations, which implies that in a local mode, all quanta are in a single bond. With only one bond at a time in motion, the pure local mode spectrum of a polyatomic molecule with identical oscillators mimics that of a diatomic molecule. For each mode, the energy levels in the frequently-used Morse potential[8] are

$$E(v_i) = \omega(v_i + 1/2) - x(v_i + 1/2)^2 - \frac{1}{2}(\omega - x/2). \qquad (1)$$

v_i is the number of stretching quanta in the ith mode, ω is the frequency ($\sim$ 3150 cm^{-1} for a C-H bond in benzene), and x is the anharmonicity ($\sim$60 cm^{-1} for such a bond.) The last term in Eq. (1) is a correction for the zero-point energy. If $v = \sum v_i$ quanta are shared in a molecule with noninteracting identical bond modes, the total energy is given by $E(v) = \sum E(v_i)$. Figure 1 is a sketch of the v = 0-3

3

manifolds of a generic molecule with at least three identical

oscillators. The "pure local mode" states, henceforth referred to

simply as the "local modes", are shown with heavy lines. They have a

degeneracy equal to the number of identical oscillators, and are the

lowest in energy in each manifold, lower by $2(v-1)x$ than the next

higher level. If a coupling between the oscillators exists, as

represented by V_{nm} that couples the local mode state to the next higher

state shown in Fig. 1, then the local-mode behavior becomes

weaker as the coupling increases. We note that with increasing

v, the effect of V_{nm} should decrease as the splitting $2(v - 1)x$

between the coupled states is increased. The bonds become nearly

independent of one another when $V_{nm} << 2(v - 1)x$.[5,7]

A simple spectroscopic test for the local behavior is to (a) see if

the local mode overtone transition frequencies fit the diatomic

molecule formula Eq. (1) and (b) determine whether the absorption cross

sections are proportional to the number of identical bond oscillators.

The first extensive studies of this sort were done with liquids, which

handily provided thick enough samples to measure the small cross

sections. (Typical cross sections are ~ 10^{-23} cm^2 at $v = 5$.) There

were many such experiments.[9-20] A representative one[15] was done on

toluene, which has two kinds of C-H bonds: the aryl C-H bonds attached

to the carbon ring, and the alkyl C-H bonds in the methyl group. The

experiment showed that they could be distinguished in the overtone

spectrum, which was well described by the local mode model.

The local mode overtone transitions were always broad in liquid

spectra, with features being smeared out to bandwidths of ~ 50 cm^{-1} or

more. Such broadening is due to frequent collisions (on psec

timescale), and intermolecular forces which perturb the vibrational frequencies. Consequently, only the grossest splittings in the spectra could be resolved, and there was no chance to test detailed theories of weaker perturbations and dynamics.

A particular pure local mode vibration involves only a single type of bond, but this is an oversimplification. More realistically, the local mode is perturbed by other vibrational modes. The spectroscopic manifestation of this mode mixing is sketched in Fig. 2, for three different cases. Case (a) describes the coupling of strength $\bar{w}$ between the local mode and a discrete nearly-degenerate mode. Two "eigenstates" result from such a Fermi resonance.[21] They are separated by about $2\bar{w}$, and their mode characters are mixed. This leads to the appearance of two lines in the absorption spectrum. In case (b), the local mode is effectively coupled with a number of nearby states, and consequently, its mode character is distributed into these coupled states. If the density of states is ρ, then the bandwidth of the effectively coupled states is $\Gamma \sim 2\pi|\bar{w}|^2\rho$. As a result, a thicket of sharp lines with a bandwidth of Γ should appear in the absorption spectrum. In the limit when the local mode couples with a continuum of states with $\rho\gamma_{rad} > 1$, case (c) results; the states are closer together than their radiative linewidths γ_{rad}. The absorption spectrum then shows a single broadened line with a linewidth $\Gamma = 2\pi|\bar{w}|^2\rho$.[21-25] Cases (a) and (c) represent the limits of small and large molecules, respectively, and (b) is the "intermediate case".

At this point we can further clarify what we mean by the term "local mode", and how we tell when we have found one. A mode is "local" if it is resistant to coupling with other nearly-degenerate

5

modes, in other words, if $\bar{w}$ decreases with increasing energy in such a way that Γ remains constant or decreases. Such a mode retains prominence in an absorption spectrum as v is raised. A mode which had a coupling strength $\bar{w}$ independent of v would have a huge bandwidth Γ at high energies where ρ is very large, and would not produce a detectable peak.

An alternative and widely used notion of local behavior has also been described. The prescription of Fig. 2 tells us that each transition corresponds to an excitation of a mixed state $\psi_n = a_n |LM\rangle + \sum_m b_{nm} |NM_m\rangle$ (LM $\equiv$ local mode; NM $\equiv$ normal mode.) In the pure local mode case, $a_n = 1$, $b_{nm} = 0$, and a single transition should be observed, assuming $\langle NM|\mu|0\rangle = 0$, where μ is the transition dipole moment. In the more general case, the fraction of local character in the mixed state ψ_n is $|a_n|^2$ and the transition to that state has an oscillator strength proportional to $|\langle \psi_n|\mu|0\rangle|^2 \propto |a_n|^2$. The qualitative conclusions regarding the local character of a spectrum would then depend on the time or spectral resolution of the spectrum. Consider "plucking" a C-H bond in benzene.[26-31] For a short time, the resulting oscillation looks like C-H stretching. After a long time, the C-H stretch energy is redistributed throughout the molecule and dissipated into heat. So for a short time, the vibration is "local"; if we used a broadband optical system to get the absorption spectrum, we would see a single transition. At long times, the vibration is not local; with a high-resolution system we could detect the many states that are coupled to the local mode.

Our criterion for local behavior does not require that we worry about exactly where the vibrational energy rattles around in a system.

6

Rather, the mere detection of a sharp vibrational resonance at high energy is _prima facie_ evidence of a local mode. Such a simple test can also be applied to other systems, such as solids, where such absorption features are not routinely observed.

Better local-mode spectra have been obtained with gaseous instead of liquid samples. Fourier transform, photoacoustic, and other spectroscopies have provided highly resolved (better than 0.1 cm^{-1}) local-mode spectra of "small" molecules such as substituted methanes.[32-37] From these spectra it was possible to analyze the Fermi resonances between the local mode state $|v_{stretch}\rangle$, with v C-H stretching quanta, and the state $|(v-1)_{stretch}, 2_{bend}\rangle$, comprising (v - 1) C-H stretching and two C-H bending quanta. The bending frequency, at ~1500 cm^{-1}, is roughly half the stretching frequency of ~3000 cm^{-1}, so that the two states are nearly degenerate. Typical magnitudes of coupling matrix elements of this Fermi resonance are in the tens of cm^{-1}; however, stretch-bend interactions can be as strong as 100 cm^{-1}.

Local-mode spectra of small molecules had shown features with Doppler-limited linewidths of less than 0.01 cm^{-1}. This indicates that the vibrational relaxation in these molecules, which have small vibrational state densities, is rather slow (> 0.5 nsec). The results on large molecules seemed very different as judged from the local-mode spectra of benzene obtained by Bray and Berry[38] and later by Reddy, Heller, and Berry.[39] Their spectra, reproduced in Fig. 3, covered the C-H stretching bands of v = 1-9. The v = 2-9 bands showed quasi-Lorentzian lineshapes that were very broad (Γ ~ 50 cm^{-1} FWHM.) Each band, presumably a local-mode band, was assumed to be due to a single transition. The "homogeneous" bandwidth Γ would then correspond to a

lifetime τ of ~ 100 fsec. Thus, there is qualitatively a huge contrast between the spectra of large and small molecules. A surprising feature of the results was that the bandwidth did not increase monotonically with the overtone level, but actually peaked at $v = 5$. A naive application of the Fermi Golden Rule $\Gamma = 2\pi|\bar{w}|^2\rho$ would predict a dramatic increase of Γ with energy, if the coupling $\bar{w}$ were constant. In other words, the decay rate should mirror ρ, the rapidly increasing density of vibrational states, ranges from $1000/cm^{-1}$ at $v = 2$ to $10^8/cm^{-1}$ at $v = 6$ in benzene.[38]

These benzene spectra inspired calculations of local mode dynamics and overtone lineshapes in large molecules.[6,7,26-31,38-54] Lately it has been speculated[50] that a local mode may be effectively coupled to only a few of the many nearly degenerate vibrational states. This would then limit ρ and hence the decay rate.

Serious questions concerning the details underlying the broad spectral envelopes have been raised. It is important to discover whether the large bandwidths are really homogeneous, and if not, what are the origins of the resolvable features. Spectra of small molecules in the gas phase are inherently easier to resolve because there are fewer vibrational modes, and rotational constants are larger (e.g. ~ 10 cm^{-1} for methane vs. ~ 0.2 cm^{-1} for benzene.) For large molecules, the resolution of individual rovibrational transitions in regions where vibrational bands overlap is very difficult. Even for a single vibrational band, collisional broadening approaches the ~ 0.01 cm^{-1} spacing between rovibrational transitions.[55] More sophisticated experiments are needed in order to provide better-resolved overtone spectra of large molecules.

Perry and Zewail studied crystalline benzene[56] and durene[57] (1,2,4,5 tetramethylbenzene) at 1.8°K, hoping to distinguish between homogeneous and inhomgeneous broadening in the $v = 5$ spectra. In such cold crystals, the molecules should all be in the ground rovibrational state. (Static intermolecular perturbations could occur, however.) In their spectra the ~ 100 cm^{-1} linewidths of the aromatic C-H stretches were seen to exceed those of the methyl C-H stretches (~ 25 cm^{-1}).

Cooling a gaseous sample by supersonic expansion is a favored method of reducing the spectral congestion by dramatically lowering the rotational temperature. The small density of molecules in the beam makes direct overtone absorption measurements difficult. It is, however, possible to detect overtone absorption in a beam by monitoring the products of vibrational predissociation resulting from overtone excitation. Butler et. al.[58] used laser-induced fluorescence to detect the OH radicals produced by predissociation of H_2O_2 from the $v = 6$ local O-H stretching mode.

Tetramethyldioxetane (TMDO) is a suitable choice for overtone absorption studies in a molecular beam because it produces electronically excited acetone upon predissociation, which can be easily detected. West et. al.[59] obtained the $v = 5$ spectra of its C-H stretch local mode. The spectra were dominated by a strong peak with a 90 cm^{-1} width, and appeared to be independent of the degree of cooling provided by the supersonic expansion. Recent experiments by McGinley et. al.[60] on the $v = 3$-5 bands have given similar results. They found that the $v = 4,5$ bands have some inherent structure, regardless of the temperature. This structure was interpreted as confirmation that the hydrogen atoms are not all on equivalent sites, so that their C-H bonds

have different vibrational frequencies. The stretch-bend couplings observed in substituted methanes should be present in TMDO as well. Although the structure was not completely resolved, an upper limit of 50 cm^{-1} was put on the homogeneous linewidth of each peak. Supersonic expansions are known to provide a high degree of rotational cooling, but are rather ineffective in vibrational cooling. Several vibrational states could have been populated in the molecular beams, so that their conclusion on the temperature dependence was not definitive. The origin of spectral broadening was therefore uncertain.

Let us consider here in more detail the results of Reddy, Heller, and Berry,[39] henceforth RHB, on benzene in a gas cell using photoacoustic spectroscopy. Their spectra, reproduced in Fig. 3, were analyzed from the point of view that the strongest peak in each represented a single vibrational transition to the local mode state of the C-H stretch overtone manifold. The 25-50 cm^{-1} bandwidths of these transitions were thought to be largely due to lifetime broadening (100-200 fsec.) On the other hand, the fundamental ($v = 1$) transitions are known to connect states with long lifetimes[55,61] and have very small homogeneous linewidths. The fundamental band contains three vibrational transitions as a result of a Fermi resonance between the zeroth-order C-H stretch and two combination modes with C-H bending character. At room temperature, each transition has a "rotational envelope" of 30 cm^{-1} width. RHB used a deconvolution procedure to remove the rotational contribution to the observed linewidths of the $v > 1$ bands. The resulting widths, assumed to be homogeneous, were then 23 cm^{-1} each for the $v = 2,3$ bands, and larger for higher overtones.

The presence of more than one non-degenerate vibrational transition

in an overtone band would invalidate this deconvolution procedure. At room temperature ($kT \sim 200$ cm^{-1}), $\sim 40\%$ of the molecules are vibrationally excited by thermal agitation. C-H stretching overtone transitions from the hot levels have frequencies different by a few cm^{-1} from those from the ground state. Furthermore, rovibrational bands whose centers were separated by only a few cm^{-1}, (much less than their rotational bandwidths of 30 cm^{-1}), would be difficult to resolve.

It was our goal to obtain local mode overtone absorption spectra as free of congestion as possible in order to resolve details of the vibrational structure. This we did by cooling the molecules in a supersonic beam to a rotational temperature of 5°K and using state-selective multilevel saturation spectroscopy[62]. We recorded spectra of the C-H stretching $v = 1$-3 local mode overtone bands of the benzene molecule and dimer of benzene. We found that these local mode bands are not composed of single, homogeneously broadened transitions. Instead, many vibration-rotation bands have been resolved in the spectra. The $v = 2$ band of the benzene molecule contains at least 25 vibrational transitions, the strongest of which, at 6006 cm^{-1}, has a natural linewidth below 1 cm^{-1}. Similarly, the $v = 3$ band contains at least 5 vibrational transitions; the strongest, at 8827 cm^{-1}, has a natural linewidth less than 3 cm^{-1}. (The $v = 3$ spectrum has a lower signal- to-noise ratio and hence, some weak transitions may have been missed.) The local mode description of the spectra appears to apply increasingly well as the quantum number v is increased.

The dimer spectra are similar in gross appearance to those of the monomer. Fine structure in the $v = 1$ spectrum puts a lower limit of $\sim$ 3 psec on the vibrational predissociation lifetime at $\sim$ 3000 cm^{-1} total

energy. Broadening of the rovibrational bands comprising the local mode overtone bands is observed. We interpret this broadening, which increases with vibrational energy, as being a manifestation of "site splitting" of inequivalent C-H bonds.

II. EXPERIMENTAL ARRANGEMENT

We have used two powerful techniques to reduce spectral congestion and thereby resolve the spectra: cooling of the molecular rotations, and state-selective saturation spectroscopy.

Our state-selective three-level saturation spectroscopy scheme used the "inverted Λ" configuration, shown in Fig. 4(a). The essence of state selection is this: a "probe" beam is adjusted to monitor only the population in a chosen subset of the $|g\rangle$ states. The "pump" beam is scanned through the spectral region of interest. Absorption from $|g\rangle$ to $|v\rangle$ causes the ground state population being probed to decrease, and hence, the probe signal. The change in the probe signal versus the pump frequency then gives us the desired absorption spectrum.

In Fig. 4(a), we assume that the probe beam has selected 3 states in the $|g\rangle$ manifold. Each of the states can make a transition $|v\rangle \leftarrow |g\rangle$ to the two states in $|v\rangle$. If the pump has a resolution that separates the $|v\rangle$ states but not the $|g\rangle$ states, two peaks (each containing three unresolved lines) should be expected, as shown in Fig. 4(b).

In our experiment, selective probing was accomplished by resonantly-enhanced two-photon ionization (R2PI), using the 260 nm $\tilde{A} \leftarrow \tilde{X}$ transition as the initial resonant step [see Fig. 5(a)]. The vibrational bands of this transition have been accurately

assigned,[63,64] and even the rotational structure of the vibrational

bands has been well analyzed.[65,66] It is therefore possible to

selectively probe a particular ground rotational and vibrational

state. Because of our limited probe laser resolution, we were able to

proble only a selected group of rotational states in the ground

vibrational level.

This electronic $\tilde{A} \leftarrow \tilde{X}$ transition also exists in the benzene dimer;

assignments of some vibrational features have been performed[67-69] but

the rotational analysis has not. The dimer's structure and moments of

inertia, which determine the rotational band-structure, are unknown.[70]

The wavelength needed to probe vibrational-ground-state dimers is

appreciably different from that used for monomers. This wavelength

difference, together with the use of a mass spectrometer, allowed us to

study monomers and dimers separately.

Figure 6 shows the salient components of our apparatus. Our sample

was a supersonic beam formed by passing argon at 200 torr through a

-30°C or 0°C bubbler which contained frozen benzene. It proceeded into

the 10^{-7} torr experimental chamber via a Lasertechnics[71] LPV pulsed

valve equipped with a 0.5 mm diameter nozzle, a region of differential

pumping, and a skimmer. Infrared and ultraviolet laser beams were

focused and carefully overlapped. They crossed the molecular beam

inside a set of ion extraction plates. The pulses of ions generated by

R2PI passed through a time-of-flight mass spectrometer and were

detected with a Johnston electron multiplier.[72] We used gated

integrators to average the ion signals for several laser shots.

Independently triggerable pulsed Nd:YAG laser systems[73] generated

the tunable UV and IR frequencies required. Each Nd:YAG oscillator-

amplifier system could generate 700-mj, 9-nsec, 9394-cm^{-1} pulses at a rate of 10 Hz. This fundamental-frequency output was frequency-doubled or -tripled, as required, in KDP crystals. Light around 38600 cm^{-1} came from a Coumarin 500 dye laser, whose output was frequency-doubled in an automatically-tracked angle-tuned KDP crystal. Infrared light came from mixing of a Nd:YAG laser beam at 9394 cm^{-1} with an IR/red dye laser beam in an automatically-angle-tuned LiNbO$_3$ crystal (WEX-1d[73]), yielding ~ 1 mj/pulse at 3000-3100 cm^{-1} and ~ 5 mj/pulse at 5800-6200 cm^{-1}. We noted experimentally that these energies were sufficient to saturate the strongest transitions in the v = 1 and v = 2 bands respectively, as predicted with the measured cross sections of RHB. We could obtain ~ 15-30 mj/pulse at 8700-8900 cm^{-1}, the region of the v = 3 band, by pumping DNDTPC dye[74] with the Nd:YAG fundamental. This was sufficient to pump ~ 10% of the molecules to be probed.

The resolution achieved with our lasers was 1 cm^{-1} in the IR and 0.3 cm^{-1} in the UV. We sometimes increased the UV resolution to better than 0.1 cm^{-1} by using an intracavity etalon in the dye laser, but the output amplitude stability was poor. By using accurately known transitions in neon optogalvanic[75] and methane photoacoustic spectra, we calibrated the laser frequencies to better than 1 cm^{-1}.

A digital computer recorded ion signal levels, scanned laser wavelengths, and actuated a shutter which was used to turn the IR beam on and off. We took special pains to overlap the foci of the IR and UV beams carefully. First we spatially filtered the UV beam with a pair of lenses and a pinhole at the focus between them. This pair of lenses also served as a telescope for adjusting the divergence of the UV beam, whose diameter was ~ 25 mm at the output lens, which had a focal length

of 35 cm. We then also installed a telescope in the IR beam to give it an adjustable divergence and increase its diameter to ~ 30 mm at the output lens of the telescope. The alignment procedure was first to adjust the beam divergences to get the foci of the two beams nearly overlapped, then set the UV beam waist to the best location for ion extraction in the molecular beam, and finally readjust the IR beam to have it well overlapped with the UV beam. The IR light, regardless of its wavelength, proved to be highly effective at fragmenting the mass-78 benzene ions produced by the UV pulse.[76-79] Therefore, to check the beam overlap, we fired the IR pulse just after the UV pulse and used the ion signal from the molecular beam as an indication for the beam overlap. This method is quite sensitive and effective; in our experiment, it was even necessary to attenuate the IR pulse energy to avoid saturation of the ion signal.

For data-taking, a group of rotational energy levels in the monomer or dimer ground vibrational state was selected by tuning the UV probe beam to the proper part of the 6_0^1 band. The R2PI spectrum of this band in the monomer, obtained by pressure-tuning the dye laser with a 0.1 cm^{-1} resolution, is shown in Fig. 5(b). In order to eliminate fluctuations in the probe signal due to time jitter between the UV and IR pulses, the UV probe pulse was delayed by ~ 15-20 nsec with respect to the IR pulse. This guaranteed that the molecules received full IR pumping before being probed. Closing and opening the shutter in the IR beam every few seconds and recording the modulation amplitude of the probe signal as a function of IR pump frequency gave us the IR absorption spectra.

The IR-pumping-induced modulation is quite small, and we were faced

with the problem of obtaining an adequate signal-to-noise ratio. Our UV laser had an intensity fluctuation of several percent and an output frequency jitter larger than the $\sim 10^{-4}$ cm^{-1} linewidths of the transitions being probed. Normalization of the ion signal to the laser pulse energy or its square was not effective in reducing the ion signal fluctuation. We needed a normalization technique which would accomodate laser frequency fluctuations as well as an arbitrary dependence of the ion signal on the laser pulse energy.

A two-beam method with identical samples was clearly mandated. We developed such a method by splitting the UV beam into two with similar powers focused on the molecular beam at two separate foci, one overlapping with the IR beam and the other not. Figure 7(a) describes the setup. The diverging UV beam struck a Suprasil flat at $\sim 45°$ incidence. The beam was S-polarized, so that $\sim 10\%$ was reflected off the front and back surfaces of the flat, which also served as the combiner for the IR and UV beams. The resulting pair of UV beams was focused at two points separated by 2 mm in the ion-extraction field of the time-of-flight mass spectrometer. The ion flight times from each of the foci to the detector were different because the foci were at different potentials. This made it possible to separate the two ion signals with time-resolved detection by gated integrators. Figure 7(b) is a schematic oscilloscope trace of the ion multiplier's output, showing that benzene ions of mass 78 and 79 [80,81] were nearly resolved in the signal from each focus. The ratio of the ion signals from the IR-pumped UV beam and its unpumped twin gave the fraction of molecules that had not absorbed IR light. (The ratio was 1 when no molecules absorbed and 0 when they all absorbed.)

16

This system worked very well in our experiment. R2PI provided well over 10,000 benzene ions/shot when the UV light was tuned to the most intense part of the 6_0^1 band. Each of the the ion signals from the two UV probes fluctuated several percent, but their ratio was constant to a few tenths of a percent, roughly the statistical limit. The resulting increase in the signal-to-noise ratio allowed us to see many weak transitions which would otherwise have been undetectable.

III. DETAILS OF STATE SELECTION -- CHARACTERISTICS OF UV AND IR SPECTRA

We wished to obtain two types of spectra in this experiment. First, we wanted to locate the vibrational transitions that make up the local mode bands. This we did with fast scans over a broad range around the RHB band centers. During these scans we did not try to resolve rotational structure within each vibration-rotation band. We call these "nonselective spectra". Then we used the state-selective technique to observe the more detailed substructure of the vibrational transitions of a smaller group of rotational states.

The coarse structure in the $\tilde{A} \leftarrow \tilde{X}$ spectrum of benzene is due to vibrational transitions from each of the thermally populated levels in the $\tilde{X}$ state (at 0, 399, 608 cm^{-1} ...) to several levels in the $\tilde{A}$ state. In an attempt to probe the ground vibrational state molecules, we chose the 6_0^1 band, which is comparatively intense and whose rotational structure has been analyzed by Callomon, Dunn, and Mills.[65] As shown in Fig. 5(a), this band occurs at 38608 cm^{-1}. No transitions from the other thermally populated vibrational levels occur at this frequency.

Since we are considering an electric dipole transition, we expect

P, Q, and R branches in the 6_0^1 band. The transition is polarized in the plane of the molecule. The selection rules on K, which is the projection of $\vec{J}$, the rotational angular momentum vector on the molecule's 6-fold symmetry axis, are $\Delta K = -1$ (p sub-branch) or $\Delta K = +1$ (r sub-branch). Consequently, there are altogether six branches of rotational transitions, labeled as $^{\Delta K}_{\Delta J}$: ^PP, ^PQ, ^PR, ^rP, ^rQ, ^rR. Their relative intensities for a given rotational ground state depend on J and K and can be computed from Clebsch-Gordan coefficients. In the limit that J,K >> 1, the ^PP and ^rR branch intensities vary as $(1/2)(1 + K/J)^2$, $^PQ,^rQ$ branch intensities $\sim(1 - K^2/J^2)$, and $^PR,^rP$ branch intensities $\sim(1/2)(1-(K/J))^2$. (Exact rotational transition matrix elements, or Hönl-London factors, are given by Herzberg.[2]) As will be discussed below, J and K tend toward parallel alignment and equal magnitude at low temperatures. This strongly favors the ^rR and ^PP branches; the ^PR and ^rP branches are so weak that they may be neglected, while the $^PQ,^rQ$ branches have medium intensity and are close together in frequency.

General trends in the PQR rotational structure can be understood with recourse to a simplified model in which the dependence on K is ignored. In this simple picture, the P branch corresponds to the real ^PP branch; the R branch is derived from the ^rR branch, and the $^PQ,^rQ$ branches are lumped together as the Q branch. The transition frequencies between the ground state with a rotational energy $B''J''(J''+1)$ and the excited state with a rotational energy $B'J'(J' + 1)$ are $\omega = \omega_0 + B'J'(J' + 1) - B''J''(J'' + 1)$. Thus, the P, Q, and R branch transitions are shifted by $(B' - B'')J''^2 - (B' + B'')J''$, $(B' - B'')J''(J'' + 1)$, and $(B' - B'')J'^2 + (B' + B'')J'$, respectively, from ω_0. A sketch of these transition frequencies vs. J" is shown in Fig. 8. Because the

18

molecule is larger in the excited electronic state, we have $B' < B''$.
It is seen that the Q branch transitions are closely grouped, slightly
to the red of the origin ω_O. The P-branch transitions have their
frequency change most rapidly with J". This makes the spacing between
transitions from different (J",K") states the largest in the P branch.
Therefore, if we want to probe simultaneously as many (J",K") states as
possible with the limited probe beam linewidth, we should tune to the Q
branch. If we want to probe only a small number of states, we should
use the P branch.

The thermal population distribution in the K levels of each J
manifold also affects the rotational state selection. For benzene, the
more accurate ground-state rotational energy is given by $B''[J''(J'' + 1)$
$- K''^2/2]$. Figure 9 is a sketch of the energy levels in this
situation. When the rotational temperature T_{rot} is low, low-energy
states with K" ~ J" are strongly favored in the distribution. This is
especially true at large J", where the rotational energy changes
rapidly with respect to kT_{rot} when K" ~ J". With only a few K" states
populated for each high J" state, and the transition frequencies most
widely spaced in the wing of the P branch, the chance to probe only a
few (J,K) states is best there.

The above discussion applies equally to the IR vibrational spectra;
the ^PP, ^PQ, ^rQ, and ^rR branches are also expected. In this case,
however, the rotational constants of the ground and excited vibrational
states do not differ substantially. With the rotational energy given
by $B[J(J + 1) - K^2/2]$, IR transitions from the heavily populated
states (J,K~J) would be expected ~ $+BJ$ from the vibrational frequency
for the ^PQ and ^rR branches and ~ $-BJ$ for the ^rQ and ^PP branches. Here

the $^rQ, ^PQ$ branches overlap the $^{PP}, ^rR$ branches because benzene is symmetric with $I_z = 2I_x = 2I_y$. This coincidence disappears when the doubly degenerate nature of the in-plane vibrations is analyzed more completely as follows.

A doubly degenerate harmonic oscillator possesses a "vibrational angular momentum"[2] and the Coriolis coupling between rotation and vibration must be taken into account. The rotational energy is then given by $E_{rot}(J,K,\zeta) = B[J(J + 1) - (K + \zeta)^2/2]$, where ζ is the Coriolis constant with $|\zeta|$ between 0 and 1. Consequently, transitions from the state (J,J) are displaced from ω_0 not by $\pm BJ$, but by $\pm B(1 - \zeta)J$ for the ^rR, ^PP branches and by $\pm B(1 + \zeta)J$ for the ^PQ, ^rQ branches. For sufficiently high J, these four branches can be well separated, as Fig. 10 with $\zeta = -1/3$ illustrates. The observed IR spectrum clearly depends on ζ. For example, when $\zeta = 0$, the Q branches are buried under the R and P branches at $\pm BJ$. If $\zeta = -1$, the Q branches coincide at ω_0, and the R and P branches are at $\pm 2BJ$. The Q branches are expected to be weak because of the $(1 - K^2/J^2)$ dependence of their intensities.

All of the above considerations for monomer spectra apply to the dimer, with some modifications. While the C-H vibrational energy level structure of the dimer is not very different from that of the monomer, there is quite an important difference in the characteristics of the rotational states: The energy levels are more closely spaced in the dimer. Without knowing whether its two constituents are able to rotate with respect to each other, it is not possible to state the selection rules for rotational transitions very well. We did not succeed in selecting a small group of rotational states during our study of the dimer. The solution of the dimer's structure and rotational spectrum

rotational spectrum appears to be a viable research problem in itself.

IV. RESULTS

A. UV Probe Spectrum

In our R2PI spectrum of Fig. 5(b) the ^PQ and ^rQ branches are not resolved. The J structure is nearly resolved in the P and R branches. Transitions from different K states provide fine structure which fills in the gaps between the intense lines from $(J,K = J)$ states. We wrote a computer program, modeled after that of Beck et. al.,[66] which calculated the absorption spectrum of the 6_0^1 band. With the rotational temperature as a variable parameter, the calculated spectrum in Fig. 5(c) appears to fit the observed spectrum in Fig. 5(b) quite well. The temperature thus determined was $T_{rot} = 5°K$. This temperature yields correctly the most intense part of the observed spectrum, but did not accurately represent the distribution in states higher than $J'' \sim 30$. The actual populations in the high-energy states are higher than those predicted from an equilibrium distribution described by T_{rot}. This is fortunate, as part of our experiment relied on probing these high rotational states.

B. Fundamental and Overtone Spectra of Benzene

Our nonselective scans were performed with the UV laser frequency tuned to the intense 6_0^1 Q branch. This gave an ion signal large enough that statistical fluctuations in the ion number were unimportant. The resulting IR spectra contain contributions from many (J,K) states and should mimic linear absorption spectra of benzene gas at 5°K. Figure 11(a) shows the spectrum in the fundamental C-H stretching region under these conditions. This is to be contrasted with the

21

fundamental band in Fig. 3. The vibrational bands of our spectrum have a FWHM of 4 cm^{-1}, consistent with T_{rot} = 5°K and the fact that "hot band" transitions are absent. The PQR rotational structure is not resolved because most of the states contributing to the signal have relatively low J values. When the UV laser was tuned to selectively probe only rotational states with high J, the rotational features in the IR spectrum could be observed.

Figure 12 shows the P-R branch splitting in the 3048 cm^{-1} fundamental C-H stretch band under different probing conditions. As the probe frequency moves further out in the wing of the P branch in Fig. 5(b), higher J states are selectively probed, and the P-R branch splitting becomes larger. The spectra are intrinsically broadened because still a group of rotational states instead of a single one was selected. They are also broadened by the finite pump laser linewidth of 1 cm^{-1}.

To within our error, the heights of the split P and R peaks in Fig. 12 are equal. This is expected since the rotational line strengths in the P and R branches should be about the same when J >> 1. By knowing the J values being probed and the splitting of the P-R branches, we can calculate ζ, the Coriolis constant. We find, for the 3048 cm^{-1} band, ζ = − 0.1 ± 0.1, in agreement with the value ζ = − .0984 ± .0023 found by Pliva.[55]

Figures 11(a), (b), and (c) show our nonselective spectra of the v = 1-3 bands, respectively. In the v = 2 spectrum, ~ 25 vibration-rotation bands have been resolved, each with a bandwidth ~ 4 cm^{-1} as in the v = 1 spectrum. Homogeneous broadening and the 4 cm^{-1} rotational envelopes contribute to these widths. Deconvolution shows that the

homogeneous broadening is less than ~ 3 cm^{-1}. Weaker bands have been emphasized by deliberately saturating the largest peak; in an unsaturated spectrum this peak has twice the intensity of its neighbor. The result here indicates that about 10 vibrational transitions are within the envelope of the most intense peak in the $v = 2$ photoacoustic spectrum of Reddy et al. (Fig. 3).

In our nonselective spectrum of the $v=3$ local mode band, only four peaks are distincly resolved. The strongest one has a FWHM of 10 cm^{-1}, which could be indicative of a single peak with 4 cm^{-1} rotational structure and ~9 cm^{-1} homogeneous broadening. However, the observed asymmetry suggests that this peak consists of at least two unresolved vibration-rotation bands, homogeneously broadened by at most a few cm^{-1}. That this is actually the case will be seen later.

The vibration-rotation transition frequencies we observed in the monomer $v = 1-3$ bands are listed in Table I. It is interesting to note that the most intense peaks in the $v = 2,3$ spectra are blue shifted ~ 10 cm^{-1} and ~ 20 cm^{-1}, respectively, from the room-temperature absorption maxima. These shifts are not expected if the only difference between the two sets of spectra is the width of the rotational envelope of each vibration-rotation band. This implies that the vibrational "hot band" transitions are responsible. The frequency of maximum intensity in the room-temperature spectrum would be between the vibrational band centers of the "hot band" and "cold band".

We can use our nonselective $v = 1-3$ spectra to assess the tendency toward local-mode behavior. Our criterion for local behavior was that the bandwidth Γ decreases or remains constant as v increases. A look at the spectra in Fig. 11 and Table I shows that the $v = 2$ band

contains many more peaks and is broader than the $v = 1$ band. This is not what we would call a local-mode-type spectrum. But in the $v = 3$ spectrum, most of the total intensity is contained in a region 10 cm^{-1} wide, and only a few other states have significant oscillator strength. This band fits our criterion for local-mode behavior.

We can even get a semi-quantitative feeling for the strengths of the interactions between the local mode and the nearly degenerate combination mode states. The calculated density of states ρ is used with the prescription of Fig. 2 to estimate the coupling strength, $\bar{w} \sim (\Gamma/2\pi\rho)^{1/2}$. The $v = 1$ band is a famous case of a "Fermi resonance" between the C-H stretch ν_{20} and the combination modes $\nu_8 + \nu_{19}$ and $\nu_1 + \nu_6 + \nu_{19}$. We use Fig. 2(a) to analyze this situation. From the separation between the peaks we find $\bar{w} \approx 25$ cm^{-1}. The $v = 2$ spectrum of Fig. 11(b) can be analyzed with the help of Fig. 2(b). With $\rho \sim 10^3/cm^{-1}$,[38] the observed width $\Gamma \approx 30$ cm^{-1} leads to a value $\bar{w} \sim 0.07$ cm^{-1}. For the $v = 3$ band, in Fig 13(c) we have $\rho \sim 10^5/cm^{-1}$,[38] and $\Gamma \sim 10$ cm^{-1}, and hence $\bar{w} \approx 0.004$ cm^{-1}. The trend of $\bar{w}$ decreasing from 25 cm^{-1} at $v = 1$ to 0.004 cm^{-1} at $v = 3$ shows that the "local mode" description becomes increasingly appropriate with increasing v. We note that we actually have determined the coupling strengths in a manner which ignores the identities of the coupled states. Considering that anharmonic coupling strengths typically depend on the degree of vibrational wavefunction overlap, there is only a small subset of all the modes that has enough "C-H stretching character" to be able to couple very strongly with the C-H local mode. This will be considered in more detail in the Discussion.

As described earlier (see Figs. 10, 12), probing in the UV P branch

enabled us to put stricter limits on the homogeneous linewidths by selecting only a few rotational states. In the 3048 cm^{-1} v = 1 band, where homogeneous broadening was negligible, the P and R branches appeared in our spectra with widths ~ 1 cm^{-1}, limited by our laser linewidth.

Repeating this state-selection procedure on the intense 6006 cm^{-1} peak in the v = 2 band gave again the laser-limited spectral width. Thus, the homogeneous linewidths in the v=2 local mode band are also less than 1 cm^{-1}. Just as in the v = 1 spectrum, the P and R branches had equal intensities and we found ζ = -0.1 ± 0.1.

State selection of the v = 3 local mode band, with its apparently unresolved vibration-rotation band structure at 8827 cm^{-1}, presented more of a challenge. The 10 cm^{-1} bandwidth suggested that we could only hope to observe selected rotational states whose P and R transitions are separated by more than 10 cm^{-1}. To do so, we had to tune to high J states (J ~ 32) in the UV P branch. The sparse population in these states caused the probe signal to be very weak. We could increase the signal tenfold by warming the benzene reservoir from -30°C, where the saturated vapor pressure of benzene is ~ 2 torr, to 0°C, where it is ~20 torr. This did not substantially increase the rotational temperature of the molecules in the beam, as far as the population in low J states was concerned. The distribution in the high J states is apparently not described by the rotational temperature. (For T_{rot} = 5°K, the equilibrium population distribution would drop to ~ 10^{-8}% at J = 32.)

Figure 13 shows our state-selective v = 3 spectrum. Part (a), obtained with probing in the UV Q branch, depicts the nonselective

spectrum of the intense 8827 cm^{-1} peak. Part (b) shows that if probing is set at J ~ 27 in the UV P branch, the P and R transitions are resolved. With selective UV probing of the J ~ 32 states, three peaks are actually resolved as shown in Fig. 13(c). In order to resolve these peaks better, we tried to select a smaller group of (J,K) states by reducing the UV dye laser linewidth to 0.1 cm^{-1}. The observed spectrum shown in Fig. 13(d) is not very different from that in (c). This suggests that the peak width of 2-3 cm^{-1} could be dominated by homogeneous broadening, but this is an upper limit on the homogeneous linewidth since we realize that the UV probing could still have selected several (J,K) states with J ~ 32.

Our discovery of three peaks in the v = 3 spectrum is anomalous. For each vibrational transition, we expect two nearly equally intense peaks (P and R). Thus, it takes more than one vibrational transition to account for the three peaks in the 8827 cm^{-1} band. On the basis of peak shapes and intensities we suggest that the low-frequency peak consists of overlapping P branch peaks and the two high-frequency peaks come from the R branch.

C. Vibrational Spectra of Benzene Dimer

We can get more information about the C-H stretching local modes in benzene by looking at their nonselective spectra in the dimer, shown in Fig. 14(a-c). The v = 1 band shows the monomer-like absorptions; The peaks are red-shifted by 1-2 cm^{-1} compared with the monomer spectrum, and they have different relative intensities. An important feature to note is the presence of two new bands with only 2 cm^{-1} FWHM at 3014 and 3072 cm^{-1}, presumably arising from combinations with van der Waals vibrations between molecules. We shall postpone the interpretation to

a later part in this section.

The spectrum of the $v = 2$ band of the dimer is quite similar to that of the monomer, except for a ~ 3 cm^{-1} red shift. Our resolution was not sufficient for us to find new peaks arising from the van der Waals interactions between the monomer subunits. We did observe a ~ 1 cm^{-1} broadening [from FWHM = 4 cm^{-1} (monomer) to 5 cm^{-1} (dimer)] on the strong peaks, which was not seen in the $v = 1$ spectrum. The $v = 3$ spectrum of the dimer appears to contain a single peak with ~24 cm^{-1} FWHM, red-shifted ~ 4 cm^{-1} from its monomer counterpart.

It is believed that the benzene dimer has a structure with lower symmetry than the monomer. Then site splittings in the C-H stretching frequencies are expected. The spectral broadenings seen in the dimer spectra could be due to the unresolved splittings of the C-H bonds. As the bond motions become more "local" in progressing from $v = 1$ to $v = 3$, each C-H bond becomes freer to move independently and experience its own local vibrational potential, and the widths of the vibration-rotation bands should increase.

Let us now consider the $v=1$ dimer spectrum more carefully, as it has bearing on a couple of long-standing problems. First, there is the question of the vibrational predissociation lifetime. In vibrational predissociation, the C-H stretching vibration decays, imparting some of its energy to the van der Waals bond between the monomers and causing the dimer to dissociate. The strength of the van der Waals bond is estimated to be ~ 900 cm^{-1}; CO_2 laser radiation at 1037 cm^{-1} is observed to fragment the dimers.[82,83] The rates of predissociation have been estimated from the observed homogeneous linewidths. Since the weak bands at 3014, 3072 cm^{-1} have linewidths of < 2 cm^{-1} before

27

deconvolution of the laser linewidth of 1 cm^{-1}, we conclude that the predissociation lifetime from the 3014 and 3072 cm^{-1} excitations exceeds ~ 3 psec.. A similar conclusion has been inferred from experiments with CO_2 lasers at 1037 cm^{-1} [83] and from a lower-resolution study with an optical parametric oscillator.[84] It has been suggested on the basis of higher-resolution (0.1 cm^{-1}) spectra obtained by Miller that the lifetime is actually in excess of ~50 psec.[85]

The structure of the dimer is not really known. Calculations[86] have not resolved the controversy. Studies of the dimer's behavior in the $\tilde{A} \leftarrow \tilde{X}$ transition have led to the conclusions that it is roof-shaped[81] or has the monomers stacked parallel with their centers offset.[70] Molecular beam electric resonance (MBER) experiments[87,88] had shown that the dimer has a dipole moment, and its structure was thought to be T-shaped. A defensible determination of the true structure will require that a rotationally-resolved spectrum be obtained and analyzed. Although we have not done this, in principle it is possible with lasers having very narrow bandwidths. An elegant experiment in which the rotational structure in the spectrum of a dimer of aromatic molecules was actually resolved was done on s-tetrazine ($C_2N_4H_2$) by Haynam et. al.[89]

A prediction of the dimer's structure would be based on a model of the intermolecular potential, which would also predict the frequencies of the six van der Waals (intermolecular) vibrational modes. Previously-obtained spectra do not display van der Waals features clearly, so the frequencies are not known experimentally. Unfortunately, we cannot provide convincing assignments of the 3014 cm^{-1} and 3072 cm^{-1} bands; the data is insufficient. Furthermore, the

fact that the dimer $\tilde{A} \leftarrow \tilde{X}$ spectrum has not been fully assigned prevents us from stating with certainty that our IR spectrum is due only to dimers in the ground vibrational state. It is possible that the 6_0^1 probe transition is overlapped by van der Waals hot bands. This would explain why a peak is detected <u>lower</u> in frequency than the lowest-frequency monomer IR transition at 3048 cm^{-1}. If only ground-state dimers were probed, combination bands would have frequencies of the form $\nu_{monomer} + \nu_{vdw}$, which are <u>higher</u> than $\nu_{monomer}$.

V. DISCUSSION

State mixing is a key element in calculations of molecular dynamics and spectra when anharmonic couplings are present. Thus far, we have used a crude model, as described with Fig. 2, to provide a reference point for viewing the local modes. In this model, the coupling $\bar{v}$ is equally strong between the local mode and all the other modes, whose density is ρ. Our use of this model was somewhat cavalier, considering that in the spectra, there is a great deal of "lumpiness". Clearly, the vibrational modes included in ρ are not all identical. This forces the conclusion that not all states are equally strongly coupled to the local mode state. Intuitively, this is expected; states whose motions have little resemblance to C-H stretching will have only small wave function overlap, and hence small coupling with the local mode. Sibert et al.[26] used more than one "tier" of states, to take into account the different degrees of coupling with the local mode, as shown in Fig. 15. In this multitier model, C-H stretching states $|v_{CH}\rangle$ with v quanta are coupled strongly to the "first tier" of states $|(v-1)_{CH}, 2_N\rangle$, which have v-1 C-H stretching quanta and two quanta in

"normal" vibrations ν_{N1} and ν_{N2}. These "first tier" states are then coupled to "second tier" states $|(v-2)_{CH}, 4_N\rangle$, and so on. Inclusion of more than three tiers is theoretically possible, but computationally difficult.

The inhomogeneous bandwidths of the $v = 5-7$ local modes of benzene calculated by Sibert et al. to be ~ 50 cm^{-1}, are not very different from the RHB experimental values. Such a width is, however, quite large compared with our 10 cm^{-1} bandwith of the $v = 3$ band. If the local mode behavior persists with increasing v, we would expect the experimental $v > 3$ band envelopes not to exceed 10 cm^{-1} in width. This would contradict the theoretical results. To be certain, spectra for the $v = 1-3$ bands should be calculated using Sibert's model.

There are two obvious shortcomings in Sibert's model which could be remedied. First is the neglect of anharmonic potential (as opposed to kinetic) coupling. This was justified on the basis of small anharmonic terms in the vibrational force field calculated by Pulay et al[90], but has not been experimentally verified. The second is the omission of cubic couplings (kinetic or potential) of the form $\langle v_{CH}|H_{LN}|(v-1)_{CH}, 3_N\rangle$. They could be significant as, for example $|1_{CH}\rangle$ (ν_{20}) is nearly degenerate and effectively coupled with a $|3_N\rangle$ state composed of the normal modes ν_1, ν_6, and ν_{19} of benzene.

Another approach to the problem of LM behavior is to consider the time evolution of a vibration which is initially a pure C-H stretch of a single bond. The rate of vibrational relaxation in such a situation is of crucial interest in the study of unimolecular reactions. By using computers, quasiclassical trajectory calculations have been done[26-30] which purport to show the time-dependent distribution of

vibrational energy in the various modes. These calculations tend to predict LM redistribution rates on the order of 10-30/psec, which translates to LM bandwidths on the order of 50-150 cm^{-1}. These results appear to be similar to those found in the multitier calculation of Sibert. Similarly, no calculation has been attempted for C-H stretch states with $v \leq 3$, but as previously mentioned, we expect that LM bandwidths should not exceed 10 cm^{-1} at $v > 3$. Thus a contradiction of the quasiclassical trajectory results is tentatively indicated. In this light, two facts are noteworthy. First, the calculated redistribution rates are quite sensitive to the details of the complete, anharmonic intramolecular potential energy surface employed. Since this surface is not yet well known, it is normally parameterized with the use of extant spectrosopic data, force field estimates, and informed guesswork. Second, the spectra of RHB[39] (Fig. 3) have been used as a test of the calculations. Relaxation rates in qualitative agreement with interpretations of these earlier spectra automatically exceed those deduced from our spectra; if a homogeneously-broadened line were observed with a 10 cm^{-1} width, an exponential decay rate of only 2/psec would be present.

It is generally difficult to calculate the local mode overtone absorption spectrum of a large, anharmonic molecule. If one used the normal-mode picture to calculate an IR spectrum for the C-H stretching overtones of benzene from combinations of C-H stretching fundamentals, three bands would be expected[44] in the $v = 2$ (6000 cm^{-1}) region. [Fundamental C-H stretches occur in a_{1g}, b_{1u}, e_{2g}, and e_{1u} symmetries. Only three pairwise combinations of these fundamentals can give the IR-active e_{1u} symmetry.] If the IR-active Fermi triad at $v = 1$ is

taken into account, seven bands[91] instead of three should show up. These numbers fall far short of the ~ 25 bands we actually observed at y = 2. Surely there are other couplings which have yet to be included to account for such a spectrum. The approach of Sibert et al. seems to be appropriate, if modifications can be made to include cubic couplings and potential as well as kinetic anharmonicity. Inclusion of potential anharmonicity will require improvement of the benzene intramolecular vibrational force field. The results of our experiment, listed in Table I, can provide part of the requisite input data concerning line frequencies and intensities for the calculation. Raman and other studies of the vibrations would help to refine the values of the anharmonic coupling constants.

Realistic calculations of room temperature spectra must include contributions from "hot" molecules. This would require an understanding of anharmonic frequency shifts and the change in local mode absorptions induced by low-frequency vibrations in the hot molecules.

Previous experiments on benzene have given results similar to ours when the question of homogeneous linewidths vs. total vibrational energy was addressed. The two-photon absorption study of the vibration-assisted $\tilde{A} \leftarrow \tilde{X}$ transition by Aron et. al.[92] on molecules in a supersonic beam showed that the lifetime broadening of the vibrational state at 6000 cm^{-1} in the excited $\tilde{A}$ state is less than ~ 3 cm^{-1}. Another molecular beam experiment by Chernoff et. al.[93] used vibration-assisted fluorescence from the $\tilde{A}$ state to study vibrational states up to ~ 10,000 cm^{-1} in the electronic ground state $\tilde{X}$. The results showed that homogeneous broadening of the fluorescent lines was limited to at most 5 cm^{-1}. In both of these experiments, most of the

32

vibrational energy appeared in the totally symmetric, ~1000 cm^{-1} "breathing mode". They suggest that this mode is only weakly coupled with other modes, since the molecule does not change its shape as the carbon ring expands and contracts.

Our experiments could be repeated with better laser sources. Nanosecond laser pulses with transform-limited linewidth (~ .001 cm^{-1}) and good amplitude stabilty are obtainable. Their application could allow single (J,K) state selection, and hence a better resolution of the vibrational transitions in the local mode bands as well as a more reliable determination of the homogeneous broadening. This would facilitate a better spectral analysis and lifetime estimates.

Of course, it is desirable to extend the study to higher overtone bands (v = 4, 5,...). To do so with our technique would require development of a tunable laser in the near IR - visible range with large pulse energies (hundreds - thousands of mj), because of the rapid decrease of the absorption cross section with increasing v, as described in Fig. 3. The peak intensity should, however, be sufficiently low in order to avoid nonlinear optical processes that may yield spurious signals, such as multiphoton electronic transitions and stimulated Raman scattering.

It is also desirable to obtain similar overtone spectra on substituted molecules. When the symmetry is lowered, it also causes some formerly forbidden transitions to become weakly allowed. In this case the study of deuterated benzenes[91,94,95] is mandated. The coupling between stretches of C-H and C-D bonds is expected to be quite weak, since the frequencies differ by ~ 1000 cm^{-1}. If couplings between identical bonds were the major hindrance to local behavior,

then local behavior is expected to appear at a lower level of excitation in partially deuterated benzene than in benzene-h_6. On the other hand, stretch-bend coupling might not be affected much. The experiments of RHB did include extensive spectroscopy of deuterated and other substituted benzenes. Their experiments should, however, be repeated in a cold molecular beam using the state-selective technique.

There are several research problems on polyatomic molecular vibrations that are related to this work. Calculations of the force fields[90,91,94,95] rely on spectroscopic data on frequencies and intensities of various vibrational transitions. Determination of the anharmonic force constants has typically been extremely difficult, and has largely been theoretical, without experimental confirmation. Our spectra provide some data to check the calculations on benzene. Likewise, the availability of a benzene dimer spectrum will facilitate calculations of the intermolecular potential.[86] Our observation of the combination bands with the van der Waals modes is especially advantageous in that respect. It is the next best thing to finding the frequencies of the van der Waals modes themselves.

VI. CONCLUSION

We have reported on what we believe to be the first high-resolution, state-selective study of local modes in a relatively large molecule -- benzene. The technique we used was a combination of rotational cooling in a supersonic beam expansion and multilevel, state-selective saturation spectroscopy. There is no doubt that the room-temperature local mode overtone spectra of large molecules previously published have had inhomogeneous congestion. Broad

"rotational envelopes" and "hot bands" appear to be the culprits.
Linear absorption measurements on room-temperature samples simply
cannot uncover the wealth of detail which is present in the spectra.

Many suspected but heretofore undetected perturbations between the
local and other vibrational modes obviously occur. Judging from the
appearances of the overtone spectra of the monomer and dimer, we
conclude that the "local mode" description of the benzene C-H stretches
applies to $v \geq 3$. Perturbation matrix elements change from ~ 25 cm^{-1}
at $v = 1$ to ~ 0.004 cm^{-1} at $v = 3$. Our linewidth measurements show
that the lifetimes of the C-H stretching vibration exceed a few psec,
even at a total energy of ~ 8800 cm^{-1}. This is in accordance with
lifetime data on other vibrational modes of benzene excited to similar
energies. In the absence of direct lifetime measurements of the local
mode states, these lifetime estimates based on the measured linewidths
are likely to be only a lower bound.

All in all, we believe that a new perspective on vibrational
relaxation rates and local mode behavior in benzene may be called for.
Our results on the local modes of the prototypical large molecule paint
a picture different from the earlier one the experimentalists have
sometimes believed in, and the theorists have strived to explain. In
that context it appears that the model of Sibert et. al.[26] has much
merit in its approach. However, as their calculation has not included
the $v \leq 3$ local mode bands we have studied, further theoretical studies
are needed.

Our measurements of the C-H stretching spectra of the benzene dimer
could help to resolve questions concerning its intermolecular
potential, structure, and vibrational predissociation lifetime. New

lines around the C-H stretching fundamental band have been observed. Certainly, the dimer's vibrational predissociation lifetime is in excess of a few psec at 3000 cm^{-1} vibrational energy.

VII. ACKNOWLEDGEMENTS

*Also associated with Department of Physics, University of California, Berkeley, California 94720.

†Also associated with Department of Chemistry, University of California, Berkeley, California 94720.

(a)Present address: IBM Almaden Research Center, 650 Harry Rd., San Jose, California 95120-6099.

References:

1. E. B. Wilson, Jr., J. C. Decius, and P. C. Cross, Molecular Vibrations (McGraw-Hill, New York, 1955).

2. G. Herzberg, Molecular Spectra and Molecular Structure. II. Infrared and Raman Spectra of Polyatomic Molecules (Van Nostrand Reinhold, New York, 1945).

3. R. Mecke, Z. Physik 101, 405 (1936).

4. B. R. Henry, Acc. Chem. Res. 10, 207 (1977).

5. M. S. Child and R. T. Lawton, Faraday Dis. Chem. Soc. 71, 273 (1981).

6. M. L. Sage and J. Jortner, Adv. Chem. Phys. 47, part I, 293 (1981).

7. M. S. Child and L. Halonen, Adv. Chem. Phys. 57, 1 (1984).

8. P. M. Morse, Phys. Rev. 34, 57 (1929).

9. R. J. Hayward and B. R. Henry, J. Mol. Spectrosc. 57, 221 (1975).

10. B. R. Henry and W. Siebrand, J. Chem. Phys. 49, 5369 (1968).

11. R. J. Hayward and B. R. Henry, J. Mol. Spectrosc. 46, 207 (1973).

12. R. L. Swofford, M. E. Long, and A. C. Albrecht, J. Chem. Phys. 65, 179 (1976).

13. M. S. Burberry, J. A. Morrell, A. C. Albrecht, and R. L. Swofford, J. Chem. Phys. 70, 5522 (1979).

14. N. Yamamoto, N. Matsuo, and H. Tsubomura, Chem. Phys. Lett. 71,

463 (1980).

15. R. J. Hayward and B. R. Henry, Chem. Phys. $\underline{12}$, 387 (1976).

16. W. R. A. Greenlay and B. R. Henry, J. Chem. Phys. $\underline{69}$, 82 (1978).

17. O. S. Mortensen, B. R. Henry, and M. A. Mohammadi, J. Chem. Phys. $\underline{75}$, 4800 (1981).

18. B. R. Henry, A. W. Tarr, O. S. Mortensen, W. F. Murphy, and D. A. C. Compton, J. Chem. Phys. $\underline{79}$, 2583 (1983).

19. M. K. Ahmed and B. R. Henry, J. Phys. Chem. $\underline{90}$, 1081 (1986).

20. M. S. Burberry and A. C. Albrecht, J. Chem. Phys. $\underline{71}$, 4631 (1979).

21. E. Fermi, Z. Physik $\underline{71}$, 250 (1931).

22. M. Bixon and J. Jortner, J. Chem. Phys. $\underline{48}$, 715 (1968).

23. F. Lahmani, A. Tramer, and C. Tric, J. Chem. Phys. $\underline{60}$, 4431 (1974).

24. K. F. Freed and A. Nitzan, J. Chem. Phys. $\underline{73}$, 4765 (1980).

25. K. F. Freed and A. Nitzan, in Energy Storage and Redistribution in Molecules, J. Hinze, ed. (Plenum, New York, 1983).

26. E. L. Sibert III, W. P. Reinhardt, and J. T. Hynes, J. Chem. Phys. $\underline{81}$, 1115 (1984); Chem. Phys. Lett. $\underline{92}$, 455 (1982).

27. E. L. Sibert III, W. P. Reinhardt, and J. T. Hynes, J. Chem. Phys. $\underline{81}$, 1135 (1984).

28. P. J. Nagy and W. L. Hase, Chem. Phys. Lett. $\underline{54}$, 73 (1978).

29. D.-H. Lu, W. L. Hase, and R. J. Wolf, J. Chem. Phys. $\underline{85}$, 4422 (1986).

30. K. L. Bintz, D. L. Thompson, and J. W. Brady, J. Chem. Phys. $\underline{85}$, 1848 (1986); Chem. Phys. Lett. $\underline{131}$, 398 (1986).

31. P. R. Stannard and W. M. Gelbart, J. Phys. Chem. $\underline{85}$, 3592 (1981).

32. H.-R. Dübal and M. Quack, J. Chem. Phys. $\underline{81}$, 3779 (1984).

33. G. J. Scherer, K. K. Lehmann, and W. Klemperer, J. Chem. Phys. $\underline{81}$,

5319 (1984).

34. G. A. Voth, R. A. Marcus, and A. H. Zewail, J. Chem. Phys. 81, 5494 (1984).

35. J. W. Perry, D. J. Moll, A. Kuppermann, and A. H. Zewail, J. Chem. Phys. 82, 1195 (1985).

36. J. E. Baggott, H. J. Clase, and I. M. Mills, J. Chem. Phys. 84, 4193 (1986).

37. A. Campargue and F. Stoeckel, J. Chem. Phys. 85, 1220 (1986).

38. R. J. Bray and M. J. Berry, J. Chem. Phys. 71, 4909 (1979).

39. K. V. Reddy, D. F. Heller, and M. J. Berry, J. Chem. Phys. 76, 2814 (1982).

40. G. A. Voth and R. A. Marcus, J. Chem. Phys. 82, 4064 (1985).

41. K. N. Swamy and W. L. Hase, J. Chem. Phys. 84, 361 (1985).

42. G. A. Voth, J. Phys. Chem. 90, 3624 (1986).

43. M. E. Kellman, J. Phys. Chem. 87, 2161 (1983).

44. L. Halonen, Chem. Phys. Lett. 87, 221 (1982).

45. G. M. Korenowski and A. C. Albrecht, Chem. Phys. 38, 239 (1979).

46. D. F. Heller, Chem. Phys. Lett. 61, 583 (1979).

47. D. F. Heller and S. Mukamel, J. Chem. Phys. 70, 463 (1979).

48. S. Mukamel and R. Islampour, Chem. Phys. Lett. 108, 161 (1984).

49. V. Buch, R. B. Gerber, and M. A. Ratner, J. Chem. Phys. 81, 3393 (1984).

50. S. Mukamel, J. Phys. Chem. 88, 832 (1984).

51. R. Bruinsma, K. Maki, and J. Wheatley, Phys. Rev. Lett. 57, 1773 (1986).

52. M. L. Sage and J. Jortner, Chem. Phys. Lett. 62, 451 (1978).

53. T. Uzer, Chem. Phys. Lett. 110, 356 (1984).

54. B. R. Johnson, R. T. Skodje, and W. P. Reinhardt, Chem. Phys. Lett. 112, 396 (1984).

55. J. Pliva and A. S. Pine, J. Mol. Spectrosc. 93, 209 (1982).

56. J. W. Perry and A. H. Zewail, J. Chem. Phys. 80, 5333 (1984).

57. J. W. Perry and A. H. Zewail, J. Phys. Chem. 86, 5197 (1982).

58. L. J. Butler, T. M. Ticich, M. D. Likar, and F. F. Crim, J. Chem. Phys. 85, 2331 (1986); J. Chem. Phys. 85, 6251 (1986) (erratum).

59. G. A. West, R. P. Mariella, Jr., J. A. Pete, W. B. Hammond, and D. F. Heller, J. Chem. Phys. 75, 2006 (1981).

60. E. S. McGinley and F. F. Crim, J. Chem. Phys. 85, 5741 (1986).

61. G. M. Stewart and J. D. McDonald, J. Chem. Phys. 78, 3907 (1983).

62. Y. R. Shen, The Principles of Nonlinear Optics (John Wiley & Sons, New York, 1984), p.227.

63. T. A. Stephenson, P. L. Radloff, and S. A. Rice, J. Chem. Phys. 81, 1060 (1984).

64. G. H. Atkinson and C. S. Parmenter, J. Mol. Spectrosc. 73, 20 (1978).

65. J. H. Callomon, T. M. Dunn, and I. M. Mills, Phil. Trans. Roy. Soc. London, Ser. A 259, 499 (1966).

66. S. M. Beck, M. G. Liverman, D. L. Monts, and R. E. Smalley, J. Chem. Phys. 70, 232 (1979).

67. J. B. Hopkins, D. E. Powers, and R. E. Smalley, J. Phys. Chem. 85, 3739 (1981).

68. P. R. R. Langridge-Smith, D. V. Brumbaugh, C. A. Haynam, and D. H. Levy, J. Phys. Chem. 85, 3742 (1981).

69. K. H. Fung, H. L. Selzle, and E. W. Schlag, J. Phys. Chem. 87, 5113 (1983).

70. K. S. Law, M. Schauer, and E. R. Bernstein, J. Chem. Phys. <u>81</u>, 4871 (1984).

71. Lasertechnics Inc., Albuquerque, New Mexico.

72. Johnston Laboratories, Towson, Maryland.

73. Quanta-Ray (Spectra-Physics, Inc.), Mountain View, California.

74. Exciton Chemical Co., Inc., Dayton, Ohio.

75. J. R. Nestor, Applied Optics <u>21</u>, 4154 (1982).

76. A. P. Simonov, G. A. Abakumov, V. T. Yaroslavtzev, V. A. Lundrev, and E. A. Fedorov, Laser Chem. <u>5</u>, 275 (1985).

77. B. S. Freiser and J. C. Beauchamp, Chem. Phys. Lett. <u>35</u>, 35 (1975).

78. H. H.-I. Teng and R. C. Dunbar, J. Chem. Phys. <u>68</u>, 3133 (1978).

79. N. B. Lev and R. C. Dunbar, Chem. Phys. Lett. <u>84</u>, 483 (1981).

80. K. G. Owens and J. P. Reilly, J. Opt. Soc. Am. B<u>2</u>, 1589 (1985).

81. K. O. Börnsen, H. L. Selzle, and E. W. Schlag, J. Chem. Phys. <u>85</u>, 1726 (1986).

82. I. Nishiyama and I. Hanazaki, Chem. Phys. Lett. <u>117</u>, 99 (1985).

83. R. D. Johnson, S. Burdenski, M. A. Hoffbauer, C. F. Giese, and W. R. Gentry, J. Chem. Phys. <u>84</u>, 2624 (1986).

84. M. F. Vernon, J. M. Lisy, H. S. Kwok, D. J. Krajnovich, A. Tramer, Y. R. Shen, and Y. T. Lee, J. Phys. Chem. <u>85</u>, 3327 (1981).

85. R. E. Miller, private communication.

86. M. Schauer and E. R. Bernstein, J. Chem. Phys. <u>82</u>, 3722 (1985).

87. K. C. Janda, J. C. Hemminger, J. S. Winn, S. E. Novick, S. J. Harris, and W. Klemperer, J. Chem. Phys. <u>63</u>, 1419 (1975).

88. J. M. Steed, T. A. Dixon, and W. Klemperer, J. Chem. Phys. <u>70</u>, 4940 (1979).

89. C. A. Haynam, D. V. Brumbaugh, and D. H. Levy, J. Chem. Phys. <u>79</u>,

1581 (1983).

90. P. Pulay, G. Fogarasi, and J. E. Boggs, J. Chem. Phys. $\underline{74}$, 3999 (1981); P. Pulay, J. Chem. Phys. $\underline{85}$, 1703 (1986).

91. S. Brodersen and A. Langseth, Mat. Fys. Skr. Dan. Vid. Selsk. $\underline{1}$, 1 (1956).

92. K. Aron, C. Otis, R. E. Demaray, and P. Johnson, J. Chem. Phys. $\underline{73}$, 4167 (1980).

93. D. A. Chernoff, J. D. Myers, and J. G. Pruett, J. Chem. Phys. $\underline{85}$, 3732 (1986).

94. S. N. Thakur, L. Goodman, and A. G. Ozkabak, J. Chem. Phys. $\underline{84}$, 6642 (1986).

95. A. G. Ozkabak, L. Goodman, S. N. Thakur, and K. Krogh-Jespersen, J. Chem. Phys. $\underline{83}$, 6047 (1985); J. Chem. Phys. $\underline{85}$, 2346 (1986) (erratum).

Table I. Fundamental and overtone transitions observed in the benzene
molecule.

frequency (cm^{-1})	intensity (arb. units)	remarks
$v = 1$		
3048 ± 0.5	5	"ν_{20}"
3079	4	"$\nu_1 + \nu_6 + \nu_{19}$"
3101	6	"$\nu_8 + \nu_{19}$"
$v = 2$		
5865 ± 1	1	
5873	1	
5878	1	
5882	2	
5899	3	
5908	2	
5926	4	
5934	8	
5947	6	
5957	4	
5967	2	
5974	5	
5980	5	
5987	6·	
5993	2	
6001	12	
6006	25	saturated (intensity is 17 in Fig. 13)
6018	7	
6025	3	
6035	1	
6042	2	
6051	2	
6064	2	
6113	2	
6126	1	
6135	1	
6145	1	
6156	2	
6162	2	
6171	1	
$v = 3$		
8806 ± 2	1	
8827	6	unresolved bands
8854	1	
8878	1	

FIGURE CAPTIONS

Fig. 1. $v = 0-3$ manifolds in a molecule with at least 3 identical

bonds which can share the v quanta. Each bond i has the

Morse-oscillator energy levels $E(v_i) = \omega(v_i + 1/2) - x(v_i + 1/2)^2 - (1/2)(\omega - x/2)$. The "local mode" state has all

quanta in the same bond and is the lowest in each manifold,

lower by $2(v-1)x$ than the next higher state, and is shown

with a heavy line. V_{nm} is the coupling strength between the

local mode and next nearest states. "Local" behavior can

occur when $V_{nm} \ll 2(v - 1)x$.

Fig. 2.   Modifications to the absorption spectrum of a local mode

(assumed to possess all the zeroth-order oscillator strength)

when it is coupled to (a) one state (i. e. "Fermi

resonance"); (b) several states; (c) a continuum. In each

case, $\bar{w}$ is the magnitude of the perturbation matrix element

between the local mode and the other states.

Fig. 3.   C-H stretch overtone absorption spectra of room temperature

benzene gas, reprinted from Ref. 39 with permission. Spec-

tral assignments in terms of the number of C-H stretching

quanta appear in the upper-right-hand corner of each panel,

along with $\bar{\nu}_0$, the positions (in cm^{-1}) of the band centers or

maxima. Dashed lines indicate deconvolved spectral features,

and horizontal double arrows identify FWHM bandwidths. The 30

cm^{-1} room-temperature rotational envelope is seen in the $v = 1$

spectrum, known to be composed of unresolved sharp lines.

Other authors have used these spectra to estimate

"homogeneous" linewidths of $v \geq 2$ bands.

Fig. 4.   Three-level saturation spectroscopy ("inverted Λ")

scheme. (a) ω_{probe}, tuned to resonance with the $|e\rangle \leftarrow |g\rangle$

transition, measures the population in three states belonging

to $|g\rangle$. ω_{pump} induces transitions from $|g\rangle$ to $|v\rangle$, the states

being studied. The depletes the population being probed, and

diminishes the probe signal. Scanning ω_{pump} with ω_{probe} fixed

gives the $|v\rangle \leftarrow |g\rangle$ spectrum. (b) Resulting spectrum; six

lines occur (3 $|g\rangle$ states each have transitions to 2 $|v\rangle$

states) but are not completely resolved.

Fig. 5.   (a) "Inverted Λ" double resonance scheme, as applied to

benzene. Only vibrational-ground-state molecules are probed

with resonantly-enhanced two-photon ionization (R2PI) via the

$\tilde{A} \leftarrow \tilde{X}$ 6^1_0 transition at 38608 cm^{-1}. Other thermally populated

vibrational levels which contribute to a linear absorption

spectrum are present at 399, 608, 674, and 707 cm^{-1}. Overtone

pumping decreases the population of electronic-ground-state

molecules, decreasing the probe (ion) signal. Molecules which

are not in the vibrational ground state engage in "hot band"

overtone transitions but do not contribute to the observed

spectrum. (b) High resolution R2PI spectrum of the 6^1_0 band

showing P ($\Delta J = -1$), Q ($\Delta J = 0$), and R ($\Delta J = +1$) branches.

(c) Simulated spectrum of the 6^1_0 band. The rotational

temperature is determined to be 5°K. $J'' \leq 8$ levels have the

largest populations.

Fig. 6.   Diagram of experimental apparatus. Overlapped, tunable,

focused IR (pump) and UV (probe) laser beams intersect the

pulsed molecular beam between a set of ion extraction plates.

The ion signal is mass-resolved and detected with a Johnston electron multiplier. A digital computer scans the IR wavelength, chops the IR laser beam, and records spectra.

Fig. 7.   Dual Beam Technique for eliminating laser-induced fluctuations in the proble signal. (a) Apparatus: P - source of diverging input beam. SS - beam splitter (Suprasil flat.) L - lens. Ff, Fb - foci of beams from front and back of beam splitter. P - ion extraction plates. E - extraction field. The beamsplitter forms the UV beam diverging from point P into two parallel, non-paraxial beams. The lens focuses them at different points in the ion extraction field. Ion flight times to the detector differ for the two foci. (b) Schematic oscillogram of ion multiplier output showing that the ion signals from the two foci are well separated, and that masses 78 and 79 are nearly resolved.

Fig. 8.   (a) Symmetric top transition frequencies in the P $(\Delta J = -1)$, Q $(\Delta J = 0)$, and R $(\Delta J = +1)$ branches vs. J", the ground state angular momentum. The K" dependence has been suppressed. The excited state rotational constant B' is less than B", the ground state constant. This causes a quadratic dependence of ω on J", as occurs in the $\tilde{A} \leftarrow \tilde{X}$ transition in benzene. The spacing between transitions is greatest in the P branch. The thermal rotational distribution "cuts off" at Jmax. (b) The mapping of transitions from state J_0 onto the absorption spectrum.

Fig. 9.   Energies of (J,K) rotational levels in benzene. The rotational Hamiltonian is $E(J,) = B[J(J + 1) - K^2/2]$. States

46

with K = 0 have $E_{rot} \approx BJ^2$; states with K = J, the lowest in each J manifold, have $E_{rot} \approx BJ^2/2$. At low temperatures, the states with K ~ J are most highly populated.

Fig. 10. Composite spectra of a single vibration-rotation band obtained with state-selective three-level saturation spectroscopy. Different groups of rotational states are probed in each case, and the pump frequency is scanned. (a) Probe is tuned to UV Q branch. Nearly all (J,K) states contribute to the probe signal. There are four intense branches: ^PP, ^rQ, ^PQ, and ^rR. (b) Angular momentum of probe population is increased, and branches begin to be resolved. (c) Probe population has high angular momentum J. Positions of the four IR branches depend on ζ, the Coriolis constant. In this example $\zeta \sim -1/3$. Observed linewidths always exceed ~ 1 cm^{-1}, the convolution of the pump and probe linewidths, even if a single state is probed.

Fig. 11. Nonselective spectra of benzene monomer overtone transitions to (a) v=1, (b) v=2, and (c) v=3. Absorption is in arbitrary units. Frequencies of band maxima (band center for v=1) in cm^{-1} are indicated. Error bars indicate the amplitude of the noise. FWHM bandwidths of some features are indicated.
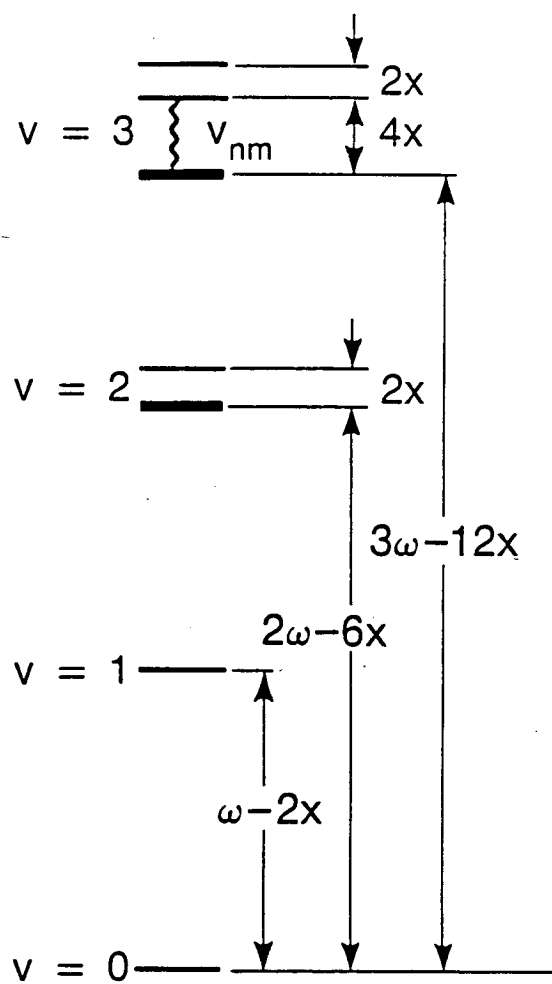
Fig. 12. Rotational-state-selective probing of the fundamental (v=1) 3048 cm^{-1} band. P and R branches are observed to separate as J'' is increased in (a) through (d). FWHM linewidths of these branches are ~1 cm^{-1}, the lower limit with our system resolution of 1 cm^{-1}. Error bars indicate the amplitude of the noise.

Fig. 13.   Spectra of intense 8827 cm^{-1} v = 3 peak with different

rotational state selection conditions. The noise level in

each spectrum is indicated with an error bar. (a) Q branch

probing of the majority of the rotational states

significantly populated in the molecular beam. (b) Probing a

group of states with J ~ 27. (c) Probing a group of states

with J ~ 32. (d) Repeat of (c) with UV dye laser in high

resolution (0.1 vs. 0.3 cm^{-1}) mode. Three peaks (two

overlapping P branches and two R branches) are observed,

showing that the peak in part (a) contains at least two

vibrational transitions.

Fig. 14.   (a-c) Nonselective spectra of benzene dimer overtone

transitions, as in Fig. 11. (a) v = 1 features at 3014 and

3072 cm^{-1} are combination bands with ~30 cm^{-1} van der Waals

stretch motions. (b,c) v = 2,3 dimer bands are broadened

with respect to those of the monomer. This would occur if

the C-H bonds were not identical in the dimer, reflecting the

dimer's lower symmetry.

Fig. 15.   Three tier scheme of Sibert et. al. for calculating local

mode spectra and dynamics. The pure C-H stretching local

mode is anharmonically coupled to combination vibrations

involving normal modes. Fermi resonance couples one C-H

stretch quantum with two normal mode quanta. The v = 6 local

mode state and the first two tiers of normal modes are

shown. "First tier" states $|5_{CH}, 2_N\rangle$ are as calculated;

"second tier" states $|4_{CH}, 4_N\rangle$ are schematic. Further tiers

are not displayed.

Anharmonic oscillator v = 0 − 3 manifolds

$2x$

$4x$

$v = 3$ ⎰ v_{nm}

$v = 2$ $2x$

$3\omega - 12x$

$2\omega - 6x$

$v = 1$

$\omega - 2x$

$v = 0$

Fig. 1

Crude model of local mode coupling with other modes
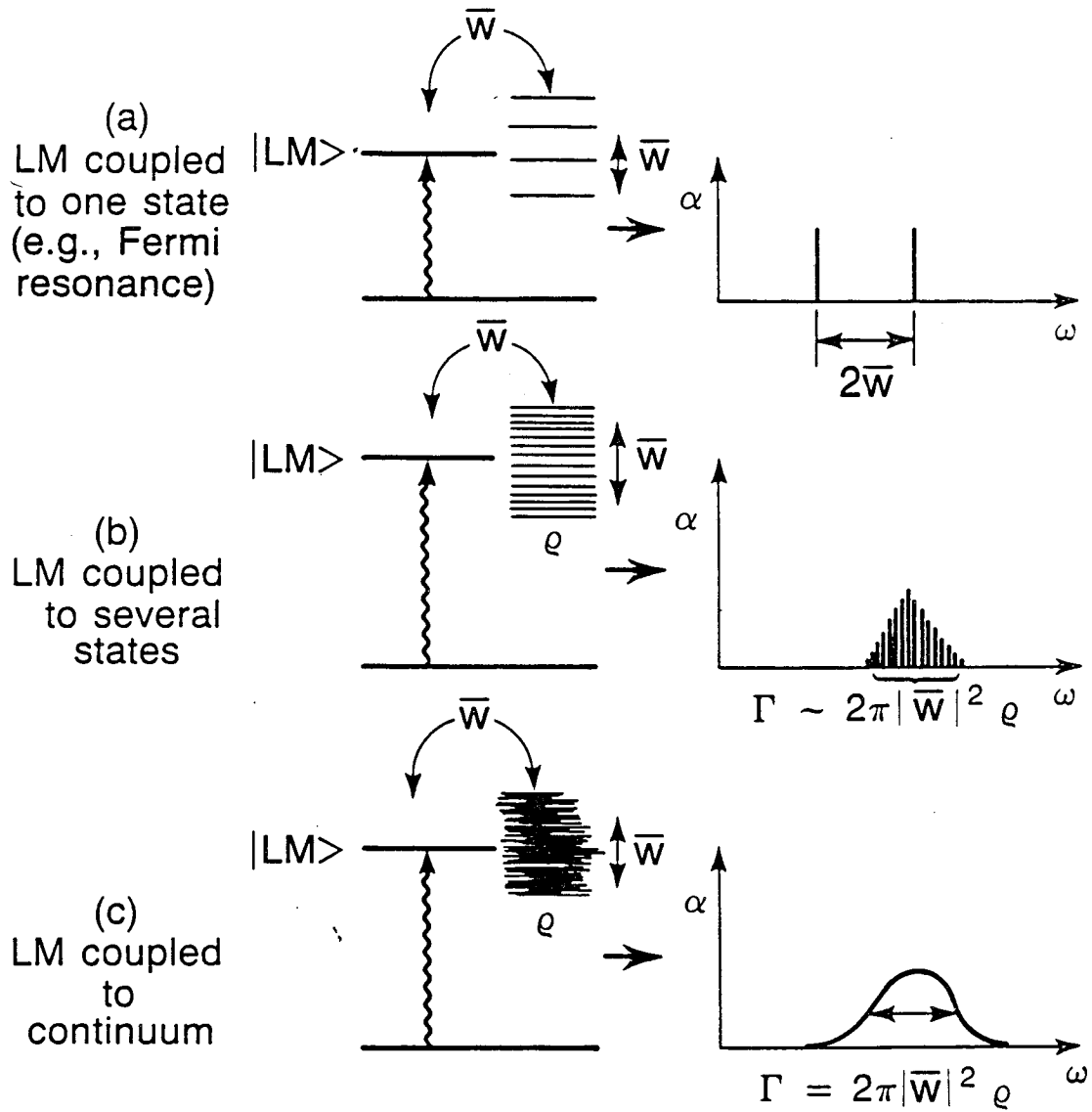
$\overline{W}$

(a)
LM coupled
to one state
(e.g., Fermi
resonance)

$|LM\rangle$

$\overline{W}$

α

ω

$2\overline{W}$

$\overline{W}$

$|LM\rangle$

$\overline{W}$

ϱ

(b)
LM coupled
to several
states

α

ω

$\Gamma \sim 2\pi|\overline{W}|^2 \varrho$

$\overline{W}$

$|LM\rangle$

$\overline{W}$

ϱ

(c)
LM coupled
to
continuum

α

ω

$\Gamma = 2\pi|\overline{W}|^2 \varrho$

Fig. 2

Room temperature absorption spectra of benzene gas

$$C_6H_6$$

Fig. 3

51

Three-level saturation spectroscopy

(a)

ω_{probe}

|e>

|v> (2 states)

ω_{pump}

Probed population —{ |g> (3 states)

(b)

Observed
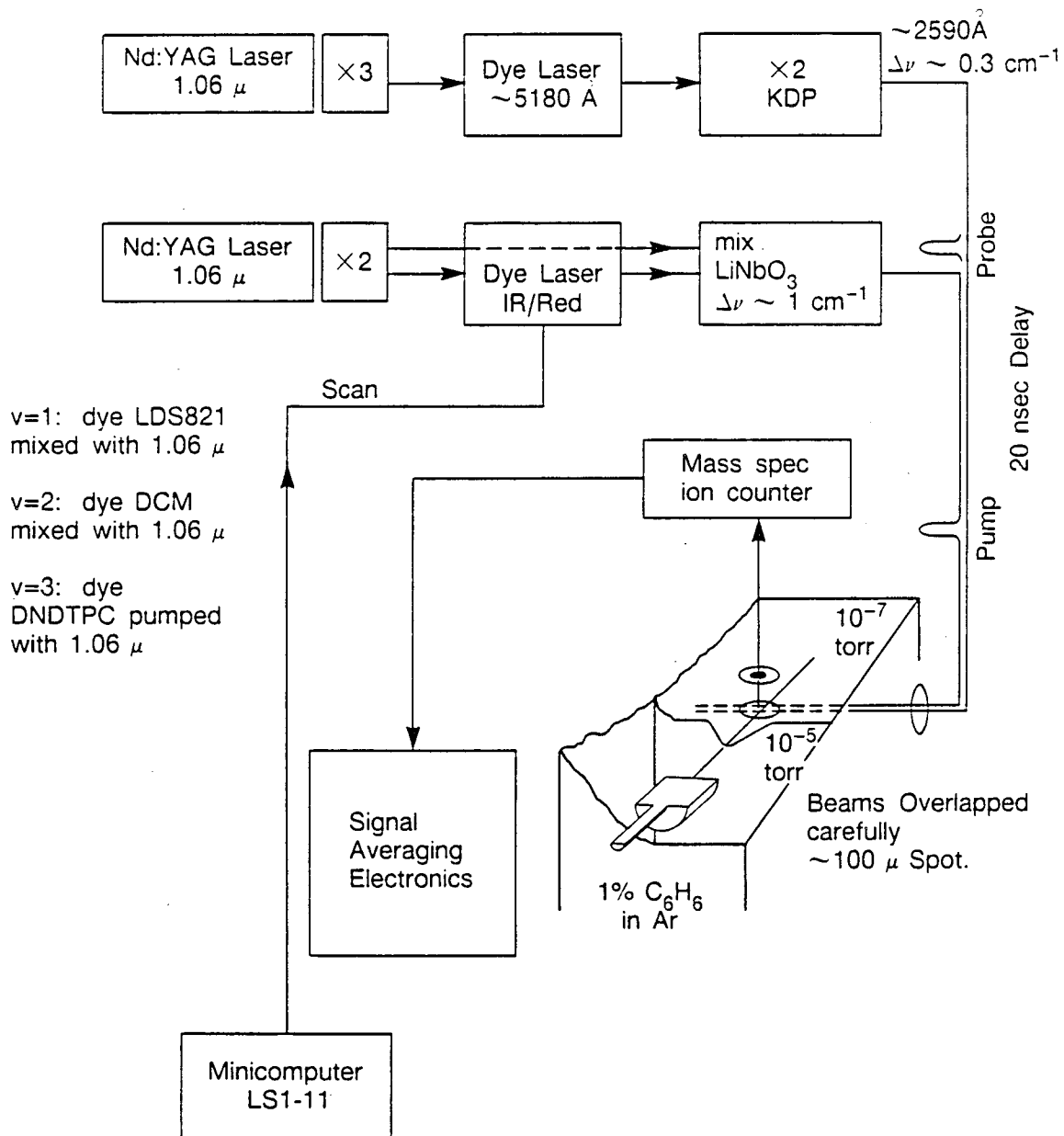v—g spectrum

Probe
signal

Pump resolution

ω_{pump}

Fig. 4

52
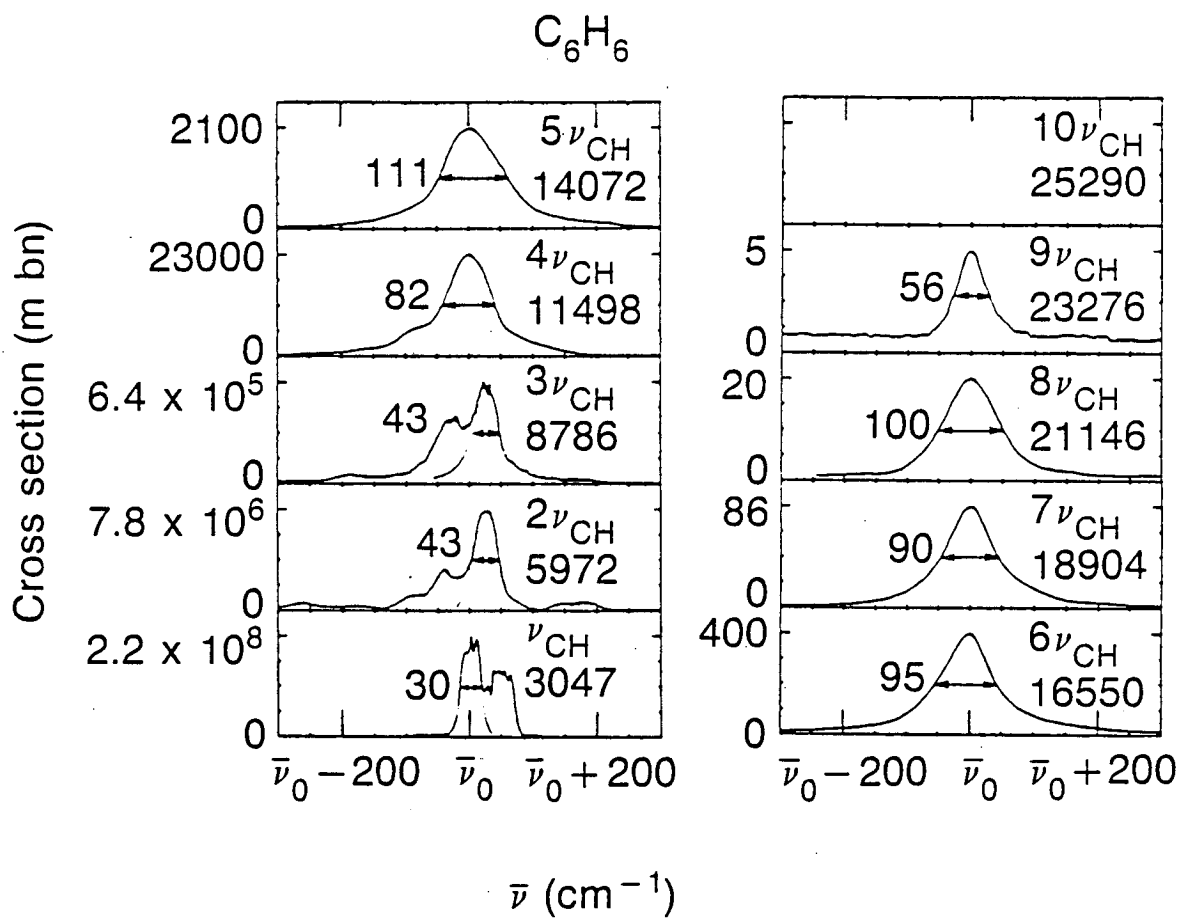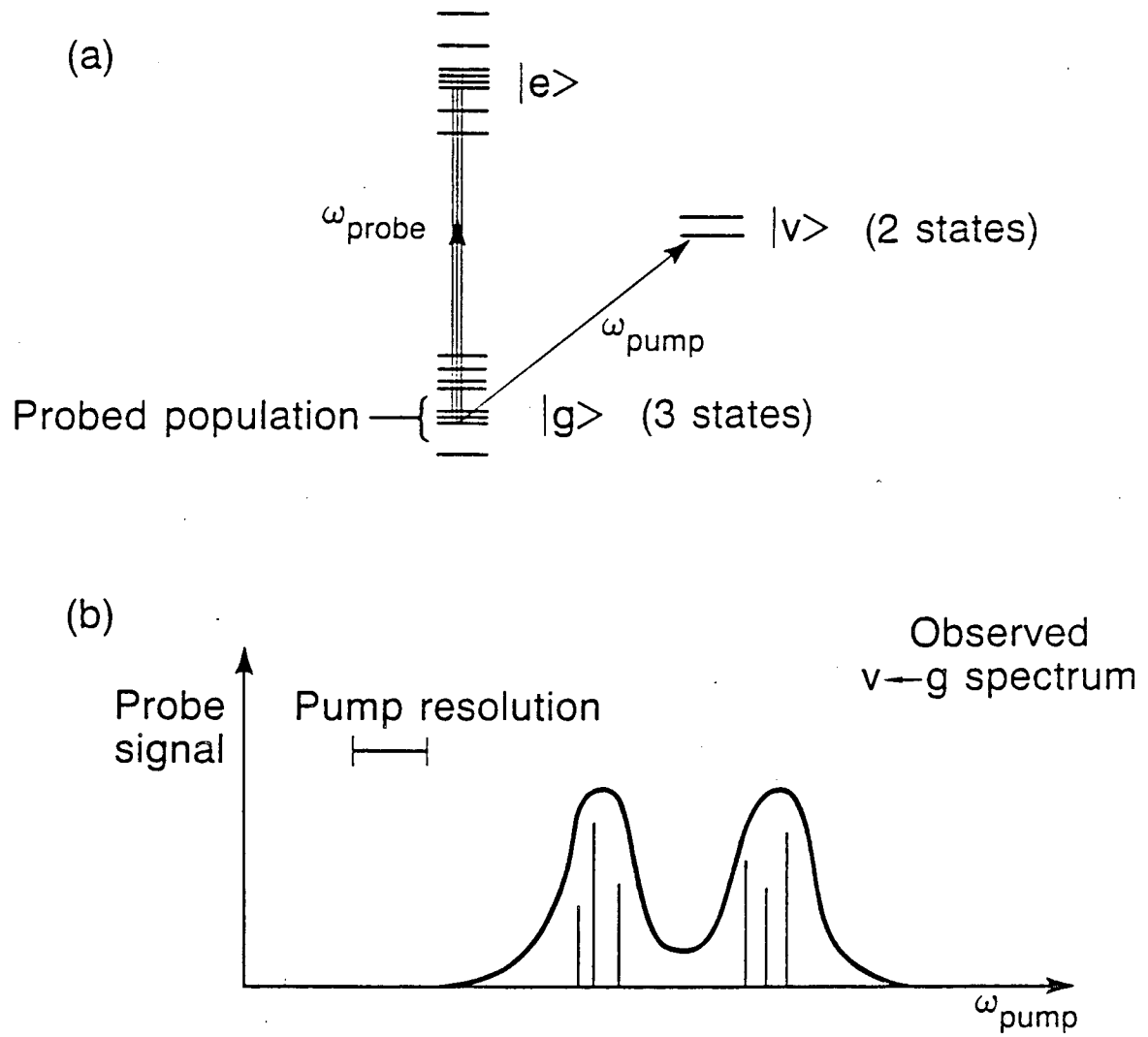
Implementation of three-level saturation spectroscopy
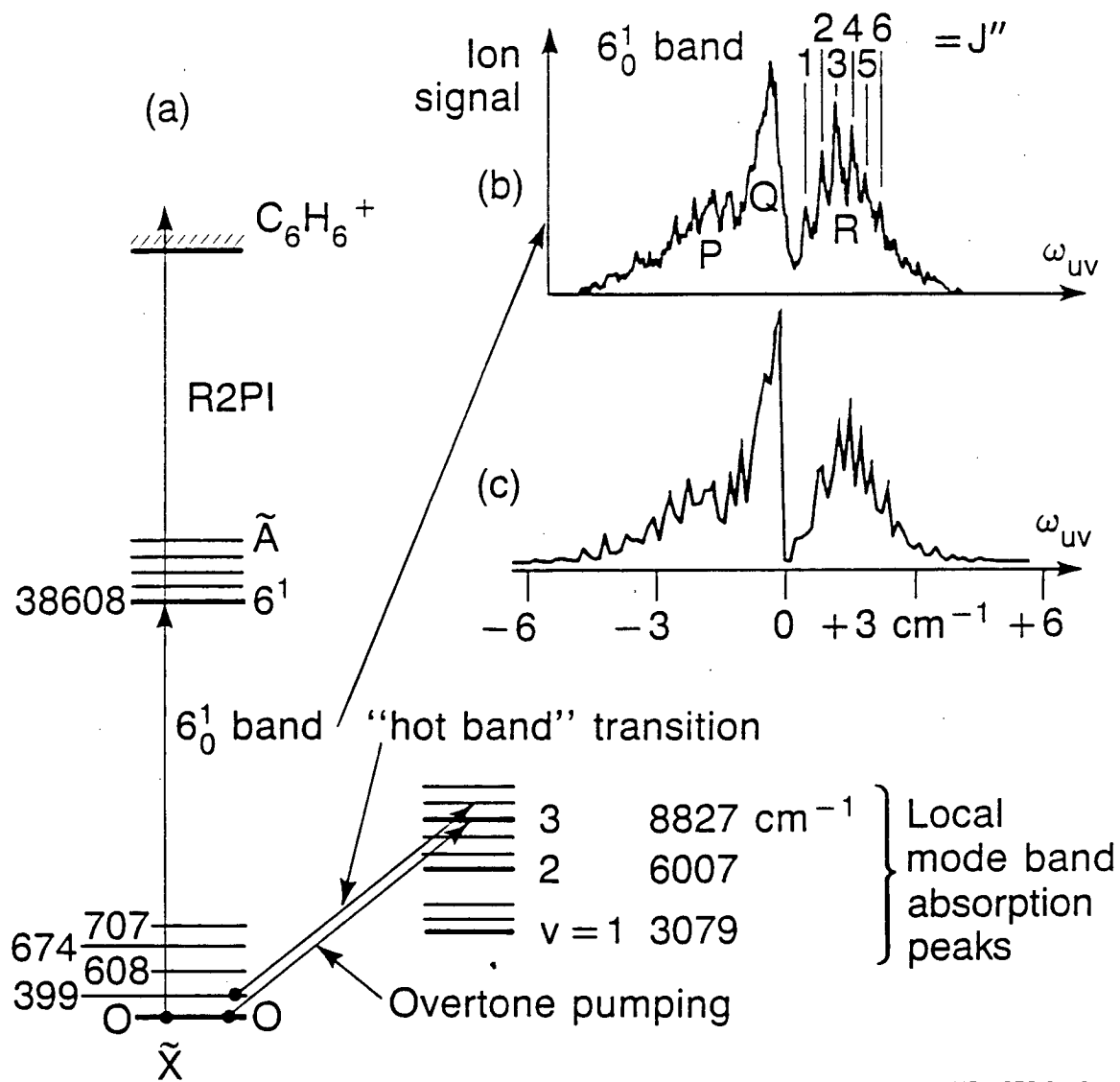
Fig. 5

Experimental Arrangement

Fig. 6

Dual beam technique

(a)

SS

F_f

$\vec{E}$

F_b

P——P

P——P

L

//// "front" beam

\\\\\ "back" beam

P

(b)

Ion signal

"back" focus

"front" focus

v

50 nsec/div

t

m/e = 78 79

Fig. 7

XBL 872-6164

55
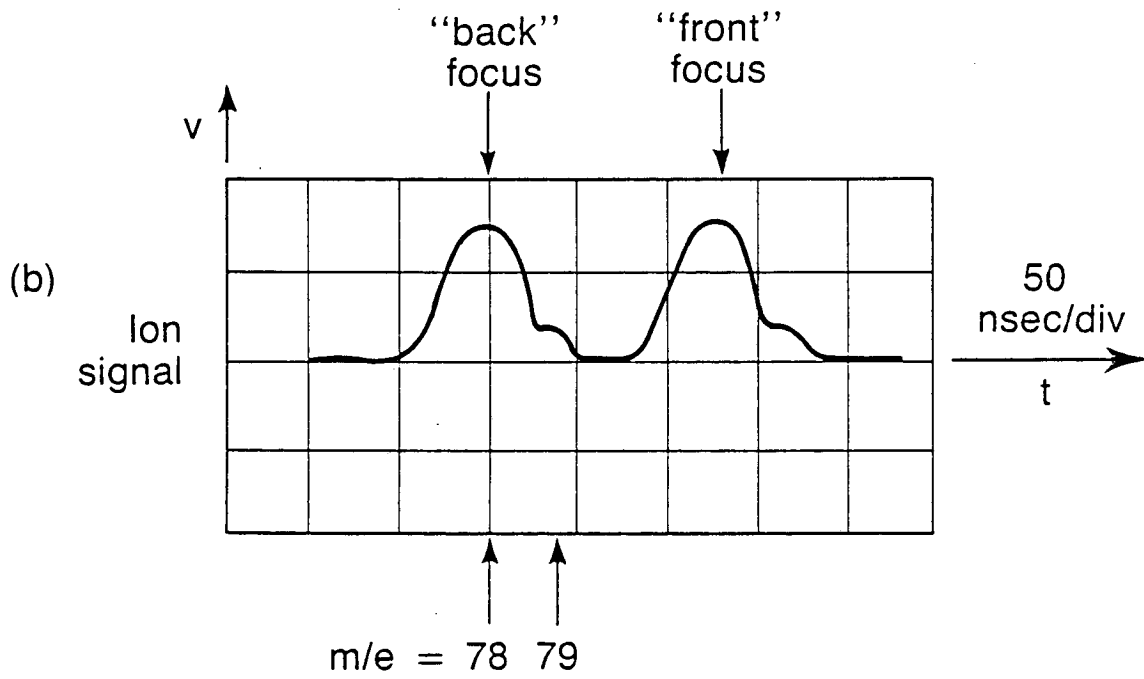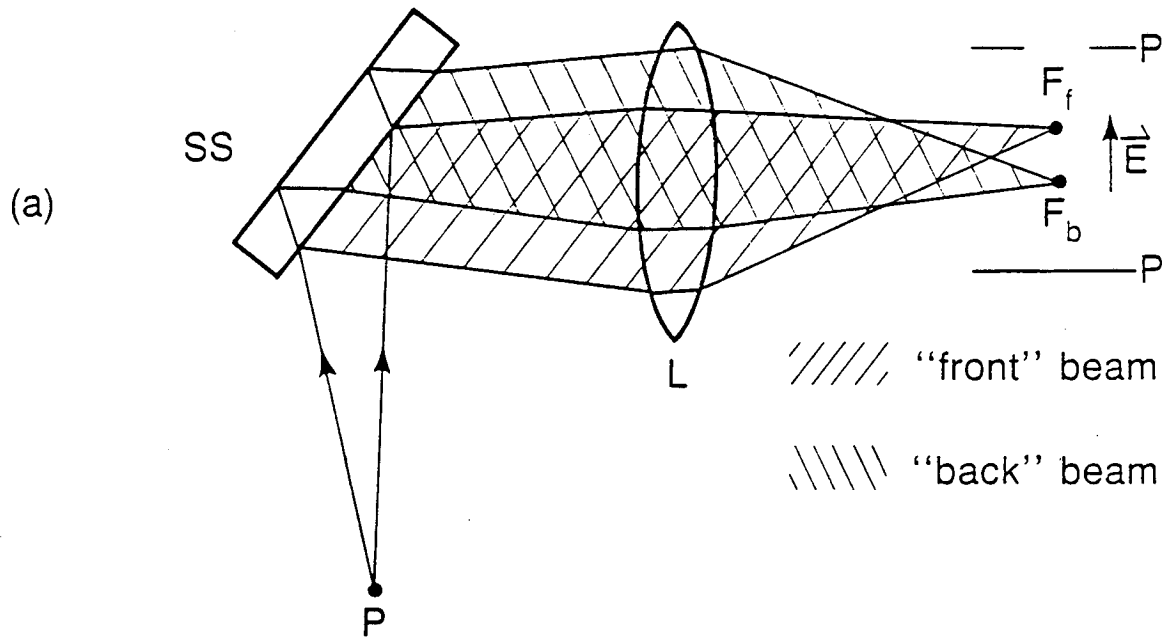
Rotational structure of "symmetric top"
electronic transition; $B' < B''$

(a)

Q ($\Delta J = 0$)

R ($\Delta J = +1$)

P ($\Delta J = -1$)

J''

J_{max}

J_0

ω

(b)

α

P

Q

R

ω

ω_0

XBL 872-6130

Fig. 8

56
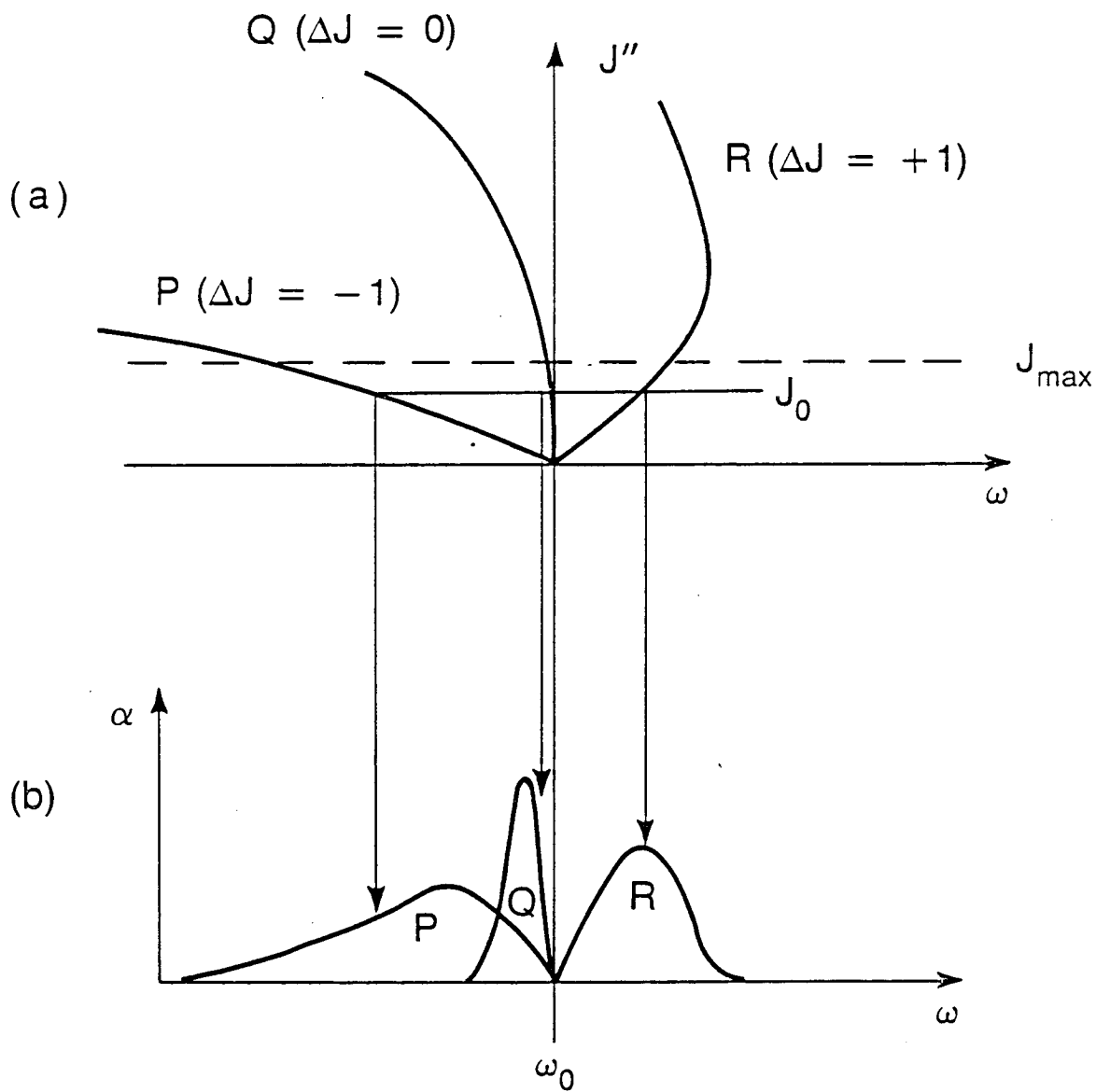
Symmetric top rotational energy levels

$E_{rot} \approx BJ^2$

$K = 0$

$\vec{J}$

$\vec{K} = \vec{J}$

E_{rot}

0
1
2
3
K = 4

$E_{rot} \approx BJ^2/2$

J = 4

J
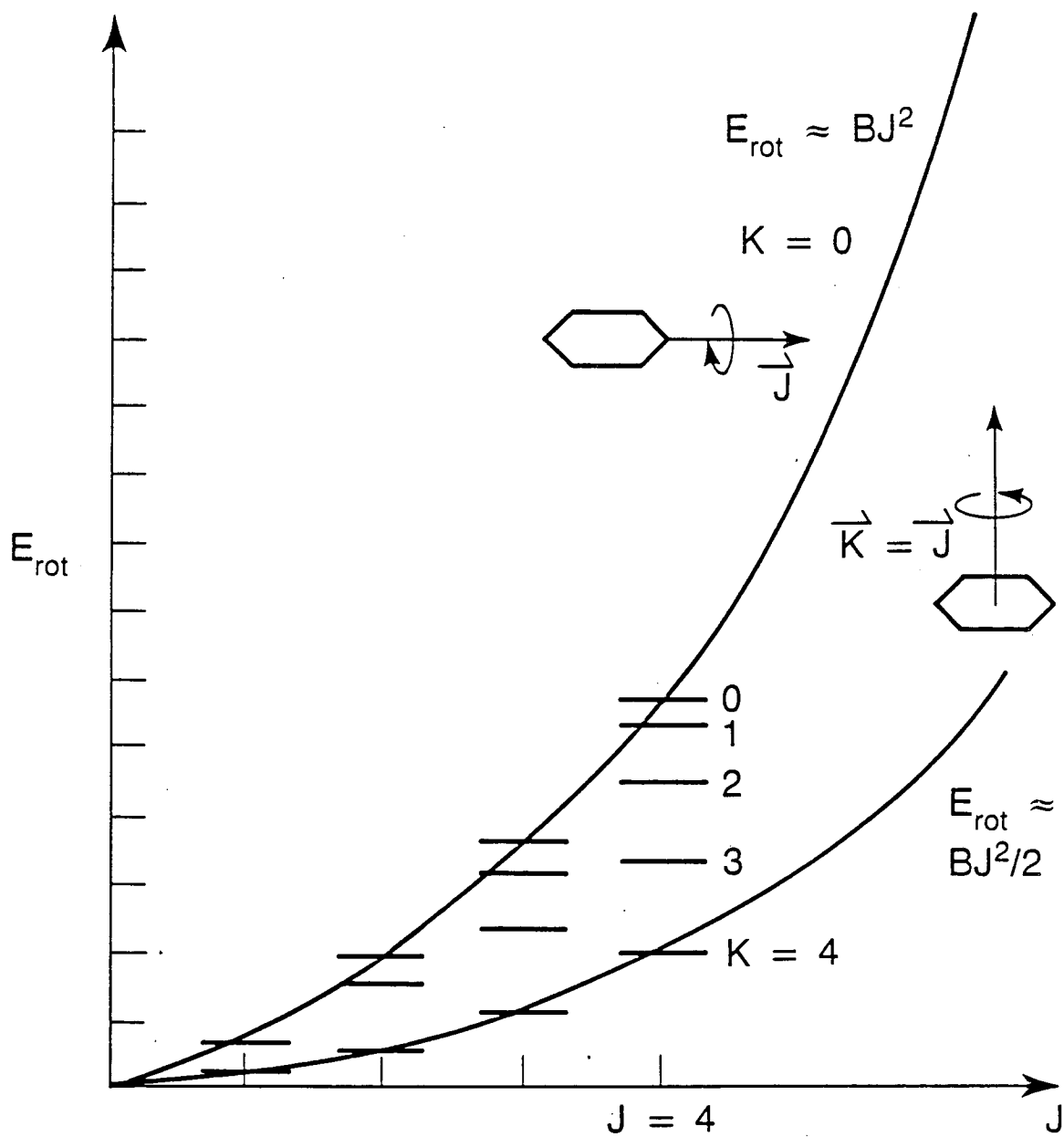
Fig. 9

Evolution of state-selective 3-level saturation
spectroscopy spectrum of a single vibrational band as
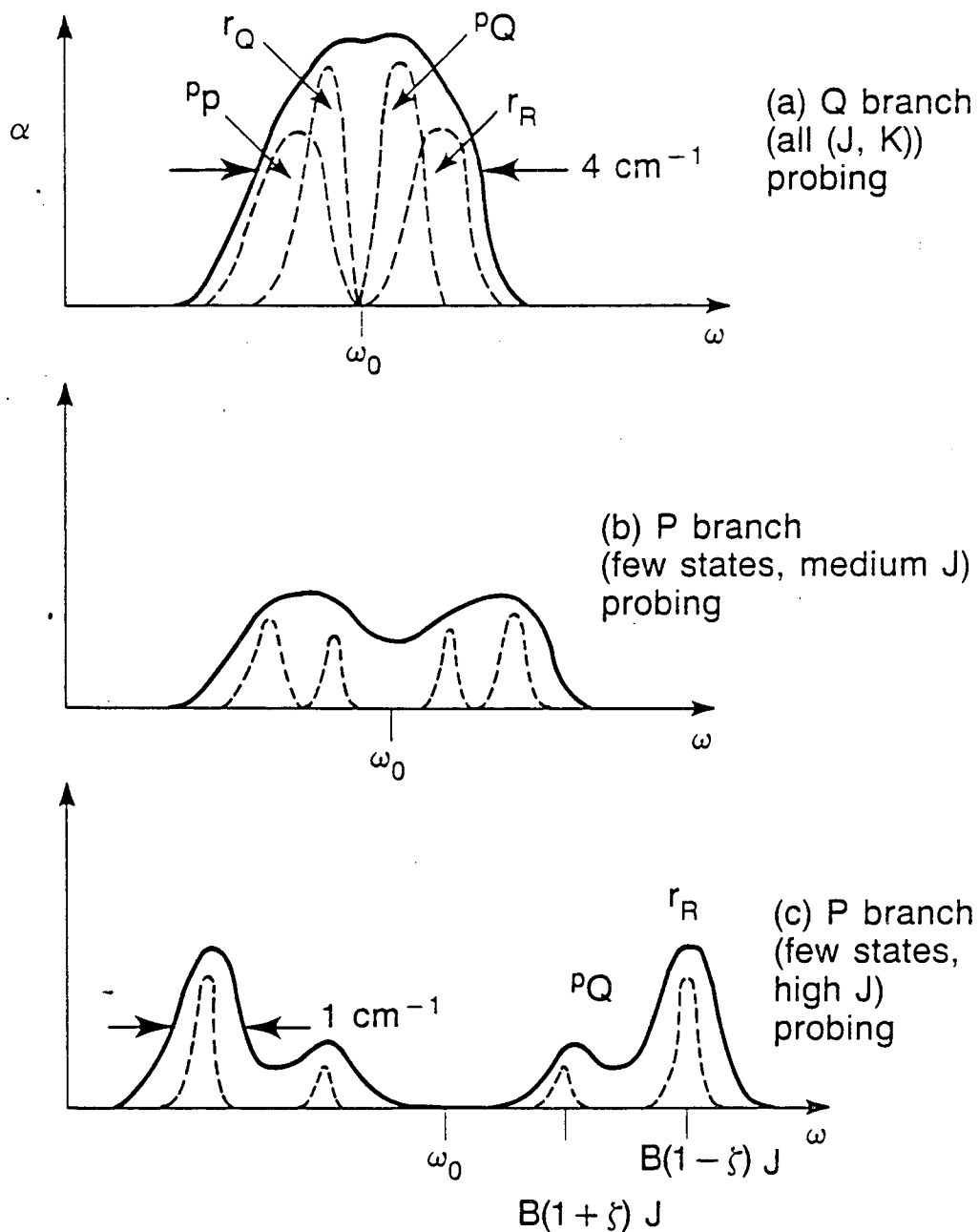different rotational states are probed

α

^rQ ^pQ

^pp ^rR

4 cm^{-1}

(a) Q branch
(all (J, K))
probing

ω

ω_0

(b) P branch
(few states, medium J)
probing

ω

ω_0

^rR

^pQ

1 cm^{-1}

(c) P branch
(few states,
high J)
probing

ω

ω_0 B(1 − ʃ) J

B(1 + ʃ) J

Fig. 10

Benzene monomer nonselective spectra

(c)

v = 3

←10 cm⁻¹

-100   8827 cm⁻¹   +100

(b)

v = 2

4 cm⁻¹

-200   -100   6007 cm⁻¹   +100   +200

3048   3101
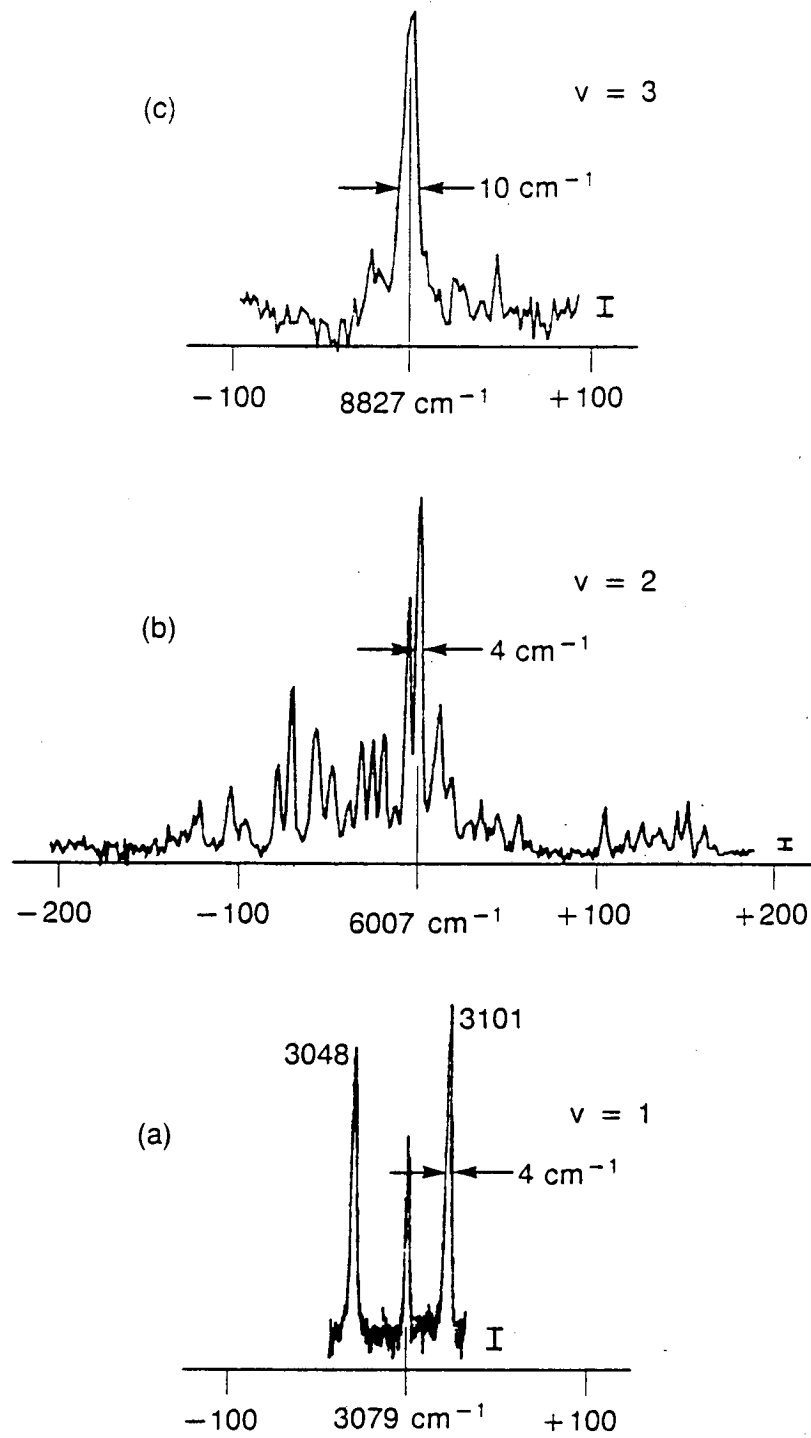
(a)

v = 1

4 cm⁻¹

-100   3079 cm⁻¹   +100

XBL-872-6146

Fig. 11

59

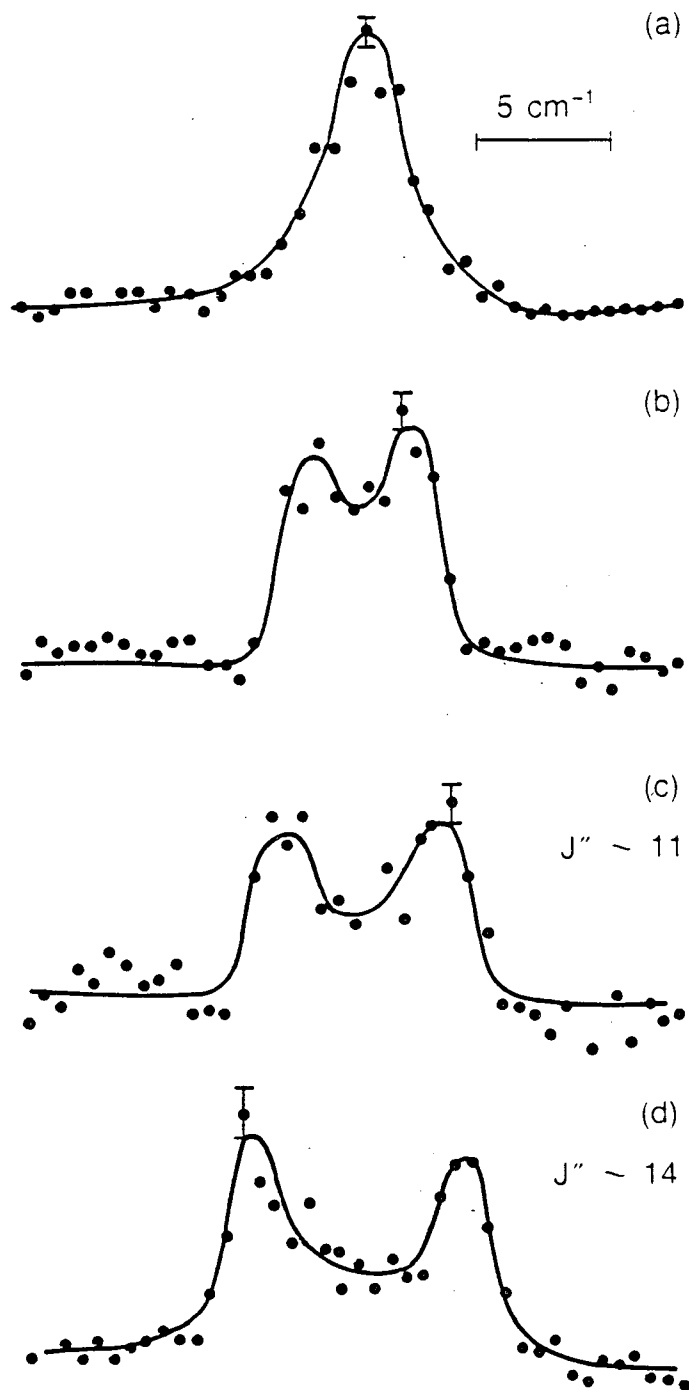## Fundamental (3048 cm⁻¹) Band Contour
with Rotational State Selection

Fig. 12

XBL 872-6169A

Benzene v = 3 Band with Rotational
State Selection

(a)

10 cm⁻¹

~ all J

8827 cm⁻¹

(b)

J ~ 27

(c)

J ~ 32

(d)

J ~ 32:
High
Resolution
Probe

XBL 872-6131A

Fig. 13

61

Benzene v = 3 Band with Rotational
State Selection

(a)

10 cm⁻¹

~ all J

8827 cm⁻¹

(b)

J ~ 27

(c)

J ~ 32

(d)

J ~ 32:
High
Resolution
Probe

XBL 872-6131A

Fig. 13

61
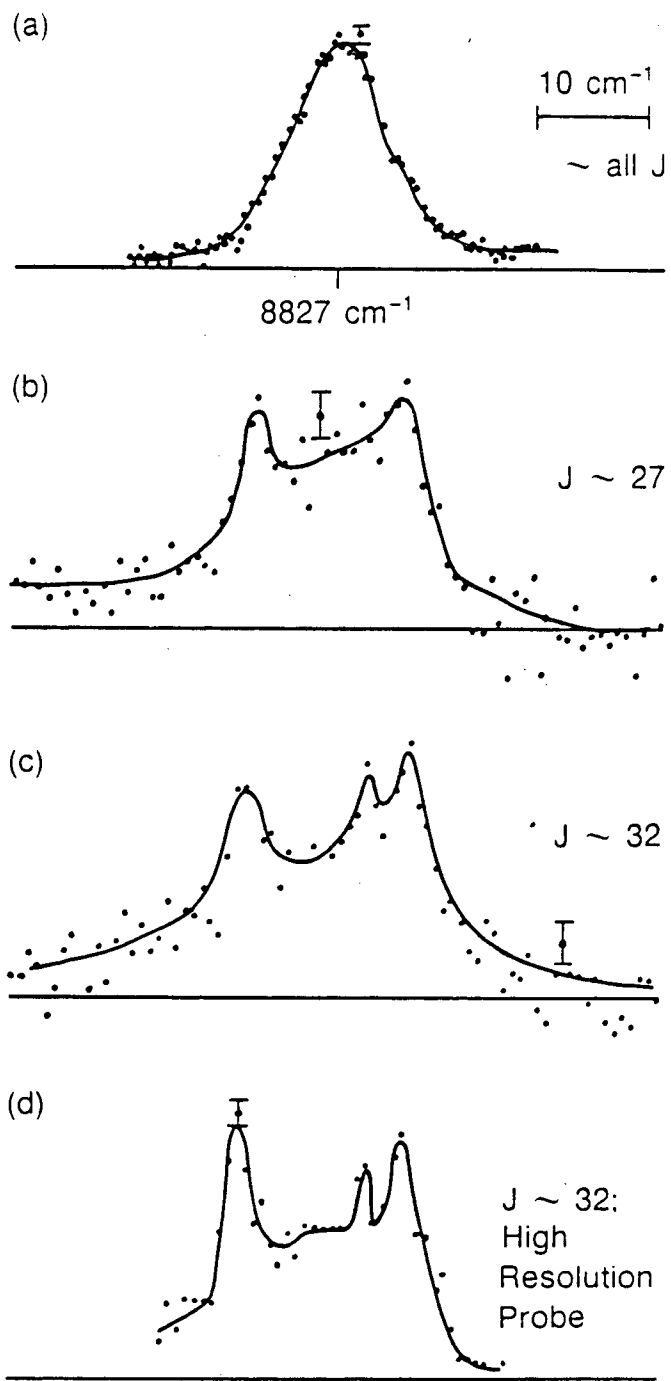
Benzene dimer nonselective spectra

(c)   v = 3

−100   8823 cm⁻¹   +100

(b)   v = 2

−200   −100   6004 cm⁻¹   +100   +200

3047   3072

(a)   3099

v = 1

3014

−100   3078 cm⁻¹   +100
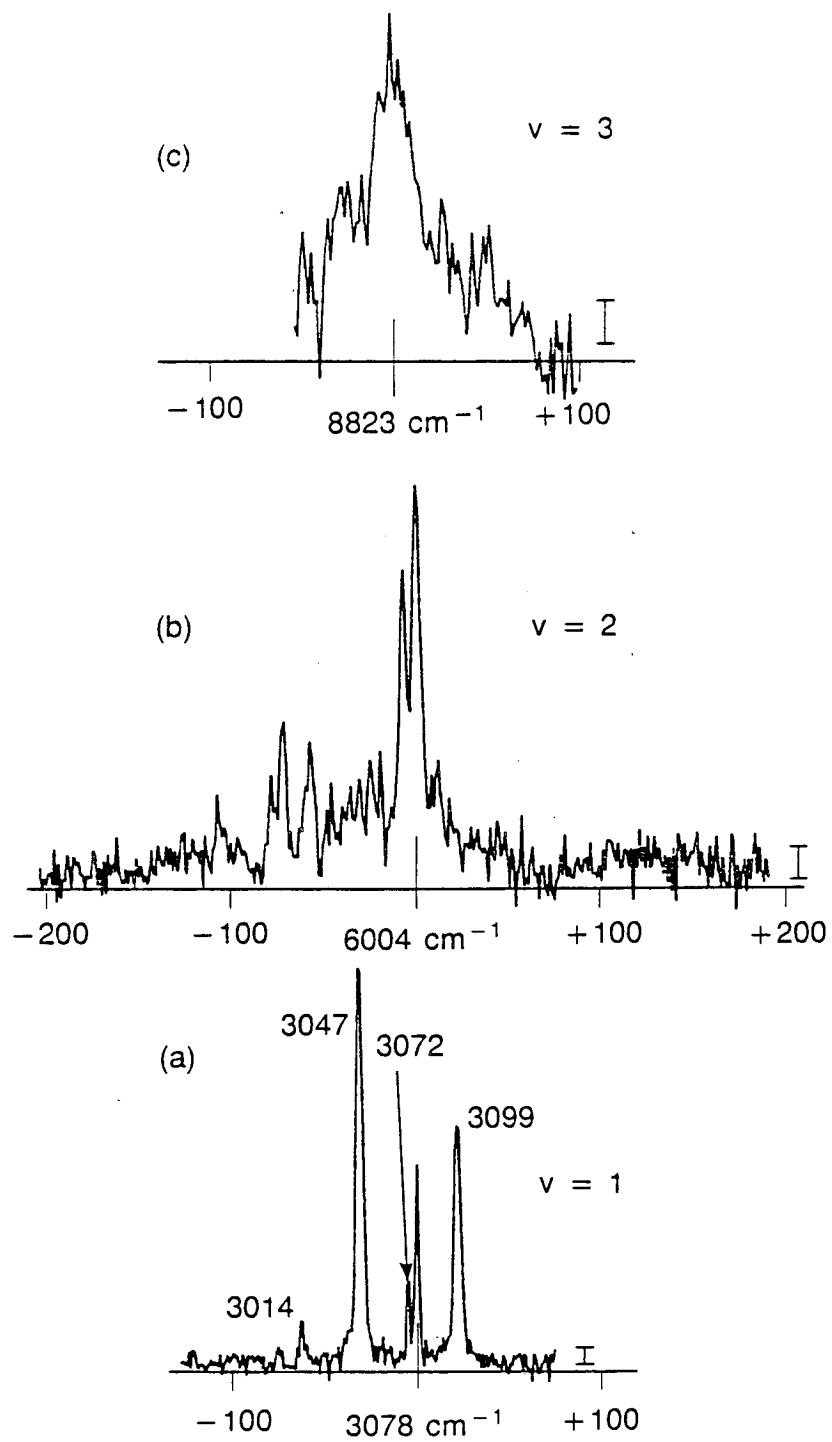
XBL-872-6147A

Fig. 14

62

Three tier coupling scheme of Sibert et al.

XBL 872-6124

Fig. 15